Scaling factors for the prediction of vibrational spectra. II. The aniline molecule and several derivatives

ARTICLE *in* INTERNATIONAL JOURNAL OF QUANTUM CHEMISTRY · JUNE 2005

Impact Factor: 1.43 · DOI: 10.1002/qua.20416

Scaling Factors for the Prediction of Vibrational Spectra. II. The Aniline Molecule and Several Derivatives

M. ALCOLEA PALAFOX,[1] M. GILL,[1] N. J. NUNEZ,[1] V. K. RASTOGI,[2] LALIT MITTAL,[2,3] REKHA SHARMA[4]

[1]*Departamento de Quimica-Fisica I, Facultad de Ciencias Quimicas, Universidad Complutense, Madrid 28040, Spain*

[2]*Department of Physics, CCS University, Meerut 250 004, India*

[3]*Department of Physics, Inderprastha Engineering College, Sahibabad, Ghaziabad, 201010, India*

[4]*Department of Physics, Meerut College, Merrut, India*

Received 8 March 2004; accepted 28 September 2004
Published online 7 March 2005 in Wiley InterScience (www.interscience.wiley.com).
DOI 10.1002/qua.20416

ABSTRACT: The structure of aniline was studied by semiempirical, ab initio, and density functional methods. Complete geometry optimization of the minimum energy structure and of the transition states for internal rotation and inversion of the amino group was carried out using several levels. The performance of the different methods in calculating and describing the vibrational frequencies of aniline was determined. The normal modes were characterized by the magnitudes and direction of the displacement vectors. Three procedures were used to obtain the scaled frequencies, two of them new, using specific scale factors and scaling equations from the benzene molecule. The errors obtained were compared with those calculated through other standard procedures. A reassignment of several bands was made. A comparison of the cost-effective method and procedure of scaling was carried out. Int J Quantum Chem 103: 394–421, 2005

Key words: aniline; structural calculations; ab initio methods; density functional methods; vibrational wavenumbers; scaling procedures

Introduction

The molecular prototype of an aromatic amine is the aniline. It has been the subject of several studies during the last two decades [1–5]. Its structure has been reported theoretically using semiempirical [6, 7], ab initio [1–6, 8], and molecular mechanics [9] methods. It is also known experimentally in the gas phase from microwave spectroscopy [10, 11] and electron diffraction [12], and in solid state from X-ray crystallography [13]. However, in all these studies there is considerable estimated uncertainty in the nonplanarity of the amino group. The structure of this amino group is important for the chemical reactivity of aromatic amines, with great chemical and pharmacological applications. A

Correspondence to: V. K. Rastogi; e-mail: v_krastogi@rediffmail.com

relationship has been established among the geometric parameters of the amino group and experimental N–H stretching vibrations [14]. Thus, the geometry of the amino group can be roughly determined and the values related to other aniline *p*-substituted. In this work we focus more attention on comparing the results from the different levels of calculations and describing the variation of the parameters with the torsion and inversion potential functions.

From a vibrational spectroscopy point of view, only one complete study of aniline was carried out, in the 1960s by Evans [15], with the assignments of the infrared spectra in the vapor, solution, and liquid phases and the Raman spectra in the liquid state. The infrared and Raman spectra of the solid state [16] and the far-infrared (IR) of the vapor phase [17, 18] were later analyzed. Theoretical prediction of the spectra using semiempirical [6], SCF and post-SCF [3, 6, 16], and density functional methods [19] have appeared in the literature. To obtain a good correlation with the experimental wavenumbers it is necessary to correct the calculated harmonic wavenumbers. For this purpose, one possible approach involves the rescaling of the force constant matrix, as proposed by Meyer and Pulay [19, 20]. This procedure will certainly improve the agreement between computed and experimental wavenumbers. However, the introduction of scaling factors for the wavenumbers themselves may be preferable, apart from its simplicity, to the more indirect approach of scaling the force constants [21]. Thus, we show here two new procedures of scaling the wavenumbers. As a first step, we studied the benzene molecule [22], from which are extracted scaling factors and scaling equations to be transferred to the aniline molecule. The errors obtained were compared with other procedures. Another goal of the present work is to test the transferability of the scale factors derived for benzene to other aromatic systems and to establish the best cost-effective method and procedure of scaling.

Computational Methods

The AMPAC 5.0 and Gaussian 94 programs packages [23, 24] were used for the calculations. In AMPAC 5.0 the semiempirical procedures AM1 [25], PM3 [26], and SAM1 [27] were selected. The keywords PRECISE and FORCE were used for optimization and wavenumber calculations, respectively. The EF routine was used for minimum search. The gradient norm was lower than 0.001. In Gaussian 94, the AM1 and PM3 methods were utilized, with the option TIGHT in full optimization. Semiempirical methods were employed because they are potentially attractive for the computation of the vibrational wavenumbers of large aniline derivatives, for their inherent low computational cost.

Ab initio calculations with wavefunction-based HF and MP2 and density functional theory methods (DFT) were performed with several basis sets, but the 6-31G** was established to initiate the comparisons. In DFT methods, the Becke (B) [28], Becke's three parameters (B3) [29] exchange functional were used with three different nonlocal correlational functional: Perdew 86 (P86) [30], Lee, Yang, and Parr (LYP) [31], and Perdew and Wang 91 (PW91) [32]. For comparison purposes the SLYP and SVWN DFT methods with exchange zero [33] were utilized.

Both program packages were used in the UNIX version with standard parameters. Minimizing the energy with respect to all geometrical parameters without imposing molecular symmetry constraints optimized all the geometry. All the calculations were performed accordingly. The wavenumber calculations were carried out at the same level as the respective optimization process and by the analytic evaluation of the second derivative of the energy with respect to the nuclear displacement.

Results and Discussion

GEOMETRY OPTIMIZATION

The labeling of the atoms is plotted in Figure 1. The optimized bond lengths, in Å, obtained with the different methods and basis sets used are listed in Table I. The experimental data reported by X-ray for one of the molecules [13], by microwave [11] and by electron diffraction in gas phase [12] are shown at the bottom of the table. It is noted that the C–N bond is remarkably long calculated by MNDO and PM3, and short by SVWN and SLYP, and the C–C lengths are remarkably long by SAM1, and all in the trend C1–C2 $>$ C3–C4 $\geq$ C2–C3.

Table II collects the calculated and experimental bond angles and torsional angles, in degrees. The *tilt* angle (ε) between the nitrogen atom and the C2–C1–C6 plane, and the inversion angle (ω), supplement of the angle between the H–N–H plane and the C–N bond, are also shown. Another inver-

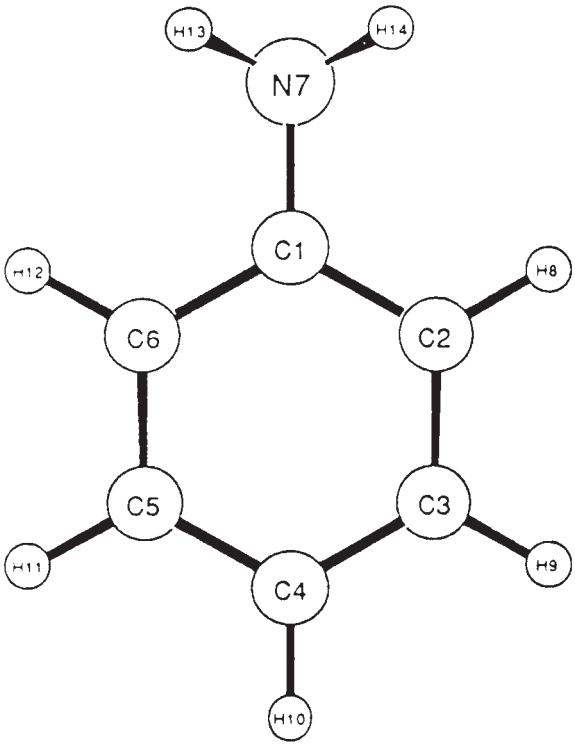

FIGURE 1. Optimum geometry of the molecule of aniline and labeling of their atoms.

sion angle γ, with respect to the benzene plane, is defined in Figure 2.

As illustrated in Figure 2. there are two possible orientations of the NH_2 plane with respect to the C–N bond axis, conformations (a) and (b). Structure (a) is the minimum energy and from this form are listed the values of Table I. It is also the conformation as revealed by X-ray [13] and by ED [12]. Structure (b) is not a minimum on the potential energy surface (0.33 kJ/mole less stable at MP2/6-311G** level), and their values were not listed. Geometry optimization starting with (b) therefore leads spontaneously back to (a).

Perhaps the most interesting structural feature of the aniline molecule, and the most difficult to determine, is the degree of nonplanarity of the amino group. The deformation from planarity (pyramidalization) of the amine nitrogen has been interpreted [2, 34] as resulting from a balance between opposing forces: the stability gained by the molecule as a whole arising from p–π conjugation of the nitrogen lone pair with the aromatic system vs. that gained by the amine using highly directed sp^3 orbital for bond formation.

As a measure of the pyramidalization [35] is defined the inversion angle ω, whose calculated value in aniline is strongly dependent on the method used. For example, it is 41.93° by AM1, close to the expected experimental value; however, by PM3 and SAM1 it is 49.46° and 31.49°, respectively, differing remarkably, especially by the failure in the calculations of the C–N bond. SVWN and SLYP also fail in the calculation of ω, with a low value the consequence of the short C–N bond determined. Experimentally, the pyramidal conformation around nitrogen is then well established, although the discrepancies observed in the extent of nonplanarity remains rather large. E.g., the values, referring to the γ angle (Fig. 2), are 37.48 ± 2° in Ref. 11 or 42.4 ± 0.3° in Ref. 10 by microwave, 38 ± 3° by X-ray [13] (43° for ω), 44 ± 4° by electron diffraction [12], 41.7° by a vibration-inversion-torsion-rotation Hamiltonian with the far-IR spectra [36], 42.17 ± 1° by vibrational analysis of the far-IR spectra [17], 42° by resonance fluorescence measurements [37, 38], and 46° by vibrational analysis of analysis of first UV band [39]. Ab initio calculations at the high level of MP2/6-311G(2d, 1p) gives a bad value for ω of 48.19°, but with the use of B3LYP/6-31G**, 41.71° was obtained, very close to the AM1 calculations and to the expected experimental value. Thus, AM1 seems to reproduce accurately the pyramidalization of the NH_2 group, similar to that obtained by B3LYP and HF, and much better than MP2, and thus it is possible to satisfactorily use this AM1 method for larger aniline derivatives. In DFT methods the increase of the 6-31G** basis set with another row of "d" functions slightly increase the pyramidalization. A satisfactory agreement was obtained in a comparison of these values with those of other authors and other levels reviewed [4, 5, 7, 34]. Only slight differences of ~2° were observed with the calculated values of Ref. 5.

The nitrogen atom is slightly out-of-plane, with a torsional angle ∠C3–C2–C1–N in the 175–180° range. As a measure of this displacement the *tilt* angle, ε, is defined, whose value is close to 3° by AM1 and SAM1, and 4.05° by PM3. With ab initio methods the value is quite insensitive to the level of calculations, varying from 2.1° by HF/6-31G* to 3.3° at the sophisticated MP2/6-311G(2df,p) [4, 40], and close to the semiempirical calculations, which confirms again the possible satisfactory use of the AM1 method for larger aniline derivatives—molecules with great pharmaceutical applications. The existence of this small *tilt* angle ε has been interpreted to be caused by asymmetric interaction be-

TABLE I

Optimum bond lengths in aniline.

Methods	C1-C2 (C1-C6)	C2-C3 (C5-C6)	C3-C4 (C4-C5)	C1-N	C2-H (C6-H)	C3-H (C5-H)	C4-H	N-H
Semiempirical methods								
MNDO	1.4190	1.4042	1.4055	1.4229	1.0909	1.0909	1.0898	1.0074
AM1	1.4148	1.3901	1.3941	1.3999	1.0999	1.1005	1.0986	0.9959
PM3	1.4020	1.3887	1.3911	1.4297	1.0964	1.0950	1.0944	0.9958
SAM1	1.4355	1.4098	1.4148	1.3929	1.0908	1.0937	1.0900	0.9946
SCF and post-SCF methods								
HF/6-31G[a]	1.395	1.389	1.389	1.401	1.072	1.072	1.070	0.997
HF/6-31G*	1.393	1.383	1.386	1.397	1.077	1.076	1.075	0.997
HF/6-31G**	1.3928	1.3831	1.3853	1.3947	1.0768	1.0763	1.0750	0.9956
HF/6-31++G**	1.3939	1.3852	1.3873	1.3953	1.0767	1.0761	1.0748	0.9959
MP2/6-31G*	1.4023	1.3942	1.3963	1.4067	1.0889	1.0877	1.0866	1.0151
MP2/6-31G**	1.4019	1.3937	1.3958	1.4056	1.0842	1.0829	1.0819	1.0103
MP2/6-311G**	1.4046	1.3965	1.3986	1.4053	1.0879	1.0867	1.0855	1.0117
MP2/6-31G(2d,1p)	1.4021	1.3953	1.3972	1.4081	1.0847	1.0834	1.0823	1.0108
MP2/6-311G(2d,1p)	1.4003	1.3928	1.3948	1.4057	1.0870	1.0855	1.0845	1.0125
Density functional methods								
SVWN/6-31G**	1.4008	1.3859	1.3907	1.3743	1.0971	1.0957	1.0940	1.0173
SLYP/6-31G**	1.4016	1.3870	1.3920	1.3728	1.1036	1.1018	1.1000	1.0231
BP86/6-31G**	1.4145	1.4004	1.4045	1.4021	1.0965	1.0954	1.0940	1.0194
BP86/6-311G(2d,1p)	1.4091	1.3954	1.3994	1.4028	1.0944	1.0931	1.0917	1.0190
BLYP/6-31G**	1.4163	1.4026	1.4065	1.4091	1.0945	1.0936	1.0923	1.0197
B3P86/6-31G*	1.4021	1.3897	1.3931	1.3925	1.0879	1.0869	1.0856	1.0111
B3P86/6-31G**	1.4022	1.3893	1.3929	1.3902	1.0872	1.0863	1.0849	1.0092
B3LYP/6-31G*	1.4052	1.3931	1.3965	1.4004	1.0881	1.0872	1.0860	1.0129
B3LYP/6-31G**	1.4054	1.3928	1.3962	1.3981	1.0875	1.0866	1.0853	1.0866
B3LYP/6-311G(2d,1p)	1.4000	1.3877	1.3911	1.3988	1.0851	1.0841	1.0827	1.0102
B3PW91/6-31G**	1.4038	1.3908	1.3943	1.3920	1.0878	1.0869	1.0856	1.0094
Experimental								
X-ray[b]	1.404 (6)	1.380 (7)	1.386 (7)	1.398 (6)	1.03 (3)	0.95 (4)	1.05 (5)	1.07 (5)
MW[c]	1.397 (3)	1.394 (4)	1.396 (2)	1.402 (2)	1.082 (4)	1.083 (2)	1.080 (2)	1.001 (10)
ED[d]	1.403 (3)	1.3933 (1)	1.3955 (1)	1.4057 (1)	1.099 (3)	1.099 (3)	1.099 (3)	1.021 (1)

[a] From Ref. 6.
[b] From Ref. 13.
[c] From Ref. 11.
[d] From Ref. 12.

tween the amino group and the benzene ring [4]. However, the X-ray value for this angle in aniline [13], 4.6, is higher than any theoretical method. This is because its value is the sum of two contributions: the electronic influence (mainly measured with the theoretical methods), and the inertial properties of the rotating NH_2 group [41, 42].

As discrepancies in Table II, the C2–C1–N angle reported by X-ray [13], 124°, is noted in complete disagreement with any other data. Slight differences are also observed in the X-ray values of C2–C3–C4 and C–N–H angles.

Because the geometrical parameters of the molecule are affected by the torsion and inversion modes [43], we carried out a study of them. Thus, Table III collects the optimized geometry in the torsion and inversion barrier height with the different methods. It is noted that in the barrier height the C–N bond is lengthening ~0.04Å in the torsion and shortening ~0.02Å in the inversion, while the

TABLE II

Calculated and experimental bond angles and torsional angles, in degrees, in aniline molecule.

Methods	C1-C2-C3 (1-6-5)	C2-C3-C4 (4-5-6)	C3-C4-C5	C2-C1-C6	C2-C1-N (C6-C1-N)	C-N-H	H-N-H	ε (*tilt* angle)	ω (inversion)	C3-C2-C1-N	C2-C1-N-H14
Semiempirical methods											
AM1	120.29	120.74	119.48	118.46	120.72	114.21	113.09	3.26	41.93	−175.48	−25.76
PM3	119.75	120.45	119.83	119.76	120.04	111.60	111.11	4.05	49.46	−175.02	−29.82
SAM1	119.46	121.14	119.30	119.52	120.20	117.82	113.64	2.82	31.49	−176.47	−20.50
SCF and post-SCF methods											
HF/6-31G**	120.39	120.88	118.74	118.71	120.62	114.64	111.35	2.16	42.30	−177.73	−25.88
HF/6-31++G**	120.38	120.88	118.73	118.76	120.60	115.00	111.56	2.54	41.28	−177.68	−25.45
MP2/6-31G*	120.43	120.58	119.13	118.84	120.49	113.09	109.74	4.17	47.03	−176.64	−29.70
MP2/6-31G**	120.43	120.56	119.16	118.84	120.47	113.01	109.77	4.37	47.18	−176.68	−30.01
MP2/6-311G**	120.55	120.54	119.12	118.67	120.56	112.80	109.70	4.31	47.70	−176.69	−30.17
MP2/6-31G(2d,1p)	120.56	120.50	119.14	118.74	120.55	112.49	109.16	3.06	48.69	−176.60	−30.31
MP2/6-311G(2d,1p)	120.61	120.50	119.13	118.64	120.61	112.60	109.61	3.38	48.19	−176.39	−29.89
Density functional methods											
SVWN/6-31G**	120.53	120.87	118.79	118.42	120.77	116.73	113.97	1.82	34.36	−177.71	−21.23
SLYP/6-31G**	120.50	120.87	118.79	118.47	120.75	116.66	114.23	1.78	34.27	−177.69	−21.06
BP86/6-31G**	120.49	120.82	118.87	118.51	120.70	114.65	111.33	2.65	42.30	−176.87	−26.26
BP86/6-311G(2d,1p)	120.55	120.78	118.89	118.45	120.73	114.02	110.78	2.92	44.23	−176.58	−27.44
BLYP/6-31G**	120.44	120.79	118.93	118.61	120.66	114.50	111.04	2.67	42.89	−176.81	−26.64
B3P86/6-31G**	120.50	120.83	118.84	118.50	120.72	115.13	111.93	2.30	40.64	−177.32	−25.11
B3LYP/6-31G**	120.48	120.80	118.88	118.56	120.69	114.84	111.50	2.38	41.71	−177.20	−25.74
B3LYP/6-311G(2d,1p)	120.53	120.76	118.90	118.50	120.71	114.23	110.90	2.74	43.64	−176.84	−27.04
B3PW91/6-31G**	120.51	120.83	118.83	118.48	120.73	115.13	111.87	2.32	40.70	−177.31	−25.17
Experimental											
X-ray[a]	119.7 (4)	122.1 (5)	117.6 (5)	117.9 (4)	124 (3)	119 (4)			43		
MW[b]	120.12 (20)	120.70 (8)	118.92 (8)	119.43 (20)	120.28 (20)	115.94	113.1 (20)[d]	4.6[e]	42.4[f]		
ED[c]	120.28 (10)	120.69 (4)	119.03 (11)	119.01 (16)	120.45 (8)				44		

[a] From Ref. 13.
[b] From Ref. 11.
[c] From Ref. 12.
[d] 111.15 ± 0.03° in Ref. 10.
[e] From Ref. 13.
[f] From Ref. 10.

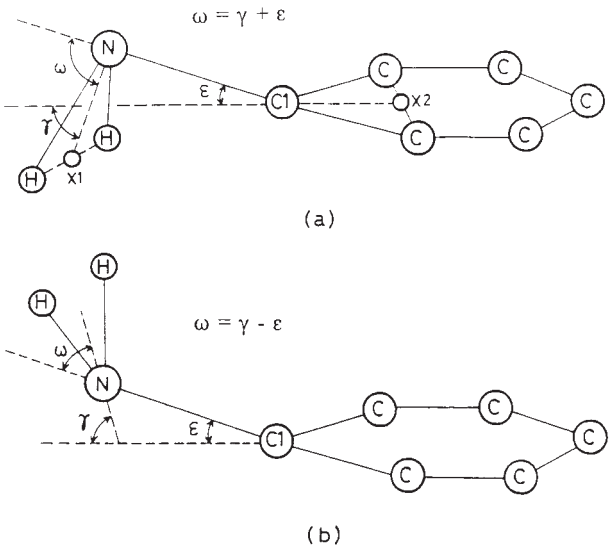

FIGURE 2. Two possible orientations of the NH_2 plane, (a) (the stable form) and (b); definition in the $-NH_2$ group of the parameters, ω (inversion angle), as $\omega = 180 - \angle X1NC1$, and ε (*tilt* angle), as $\varepsilon = 180 - \angle NC1X2$, where X1 and X2 are the points situated in the centrum of the H · · · H and C · · · C lines, respectively.

C1–C2 is slightly shorter, 0.006Å, in the torsion and slightly longer, 0.003Å, in the inversion. This is due to the fact that in the torsional barrier height the pyramidal character at the nitrogen atom is significantly incremented (i.e., the nitrogen atom is strongly sp^3-like in character), which is accompanied by a lengthening of the C–N bond. Contrarily, the planar form is accompanied by a shortening of the C–N bond.

In the angles, C2–C–N is about 2–3° lower in the torsion and almost unchanged in the inversion, while C–N–H is closing ~3° with HF and MP2 and ~5° with DFT methods in the torsion, and opening ~5° (8° in MP2) in the inversion; and similarly, the HNH angle. A remarkable increase of ω and a decrease of ε characterize the torsion.

Initially, the barrier to inversion at the nitrogen atom was estimated by Evans [15] as 4.5 Kcal/mole (18.82 kJ/mole), and the internal rotation of the NH_2 group as 3.54 kcal/mole. Later, the inversion barriers of the amino group were determined by resonance fluorescence, 454 ± 70 cm^{-1} in Ref. 37 and 509.0 cm^{-1} in Ref. 38, by UV 562 cm^{-1} in Ref. 39, and by far-IR spectroscopy in gas phase, 524.4 ± 5 cm^{-1} in Ref. 17, and 525.9 ± 5 cm^{-1} in Ref. 18. These values are very close to our HF and MP2 calculations, but slightly larger, ~1 kJ/mole, than our DFT results. The MP2 energy value seems incoherent. Our HF and MP2 barriers are in agreement with those reported in Refs. 4 and 5. It is noted in Table III that the inversion barrier by HF and MP2 methods is higher than DFT methods, while the torsional barrier is remarkably lower, about three times at the HF and MP2 level, and about 6–7 times with DFT.

In the inversion barrier height a completely planar structure of the entire aniline molecule would maximize the nitrogen lone pair-ring orbital interaction between the amino group and the ring, while in the torsional barrier height a perpendicular form of the NH_2 and the benzene ring planes minimizes this interaction [5]. Thus, the low inversion barrier and the remarkably higher rotation barrier may indicate that a small amount of π delocalization contributes more toward stabilizing the lone pair electrons than does the incremental localization of the lone pair by introducing more *s* character to the lone pair [4]. The π delocalization increases as the C–NH_2 assembly moves towards planarity during inversion. This helps to stabilize this transition state geometry relative to the global minimum, thereby lowering the inversion barrier [4].

As consequence of the variation of ω and ε with the torsion and inversion motions, they were studied in detail. Thus, in Figure 3 a is plotted (solid line) the optimum value of the inversion angle ω obtained for different torsional angles α around the C–N bond. Only HF and B3LYP with the 6-31G** basis set, and MP2 with the 6-311G** basis were used. A broken line represents the B3LYP method, the minimum of the inversion potential function for some of the torsional angles α. The numerical values for 30, 45, and 60° torsional angles are shown in Table IV. The close values determined by B3LYP and HF and the differences with the MP2 results are noted.

Conjugation of the amino group lone pair with the ring is particularly well illustrated by the lengthening of the C–N bond (Fig. 3b) and the increase of the inversion angle ω, with the torsional angle α around the C–N bond. Similar trends with the HF, MP2, and B3LYP methods are observed. It is noted that at low angles α, HF and B3LYP results are close, while MP2 differs remarkably. However, at high values of α (close to 90°), the MP2 and B3LYP results are close, while HF differs considerably.

With the rotation a closing of the HNH angle and an increment of the ω angle is observed (Fig. 3c). The relation is almost linear. The increase of ω is irregular with the increment of the torsional angle α (Fig. 3d). This can be attributed to the simultaneous

TABLE III

Calculated geometry for the inversion and torsional barriers.

	Torsional barrier							Inversion barrier					
Parameters	HF/6-31G**	MP2/6-31G*	MP2/6-311G**	BP86/6-31G**	BLYP/6-31G**	B3P86/6-31G**	B3LYP/6-31G**	HF/6-31G**	MP2/6-311G**	BP86/6-31G**	BLYP/6-31G**	B3P86/6-31G**	B3LYP/6-31G**
C1-C2	1.3865	1.3977	1.3996	1.4066	1.4084	1.3948	1.3980	1.3956	1.4075	1.4170	1.4190	1.4046	1.4079
C2-C3	1.3862	1.3962	1.3988	1.4040	1.4061	1.3926	1.3961	1.3823	1.3958	1.3997	1.4018	1.3887	1.3921
C3-C4	1.3845	1.3965	1.3987	1.4036	1.4055	1.3921	1.3954	1.3855	1.3987	1.4048	1.4068	1.3931	1.3964
C1-N	1.4319	1.4445	1.4435	1.4512	1.4588	1.4361	1.4440	1.3737	1.3790	1.3823	1.3880	1.3725	1.3787
N-H	1.0005	1.0196	1.0161	1.0277	1.0281	1.0162	1.0181	0.9894	1.0029	1.0121	1.0119	1.0030	1.0042
C1-C2-C3	120.51	120.37	120.48	120.58	120.54	120.59	120.56	120.37	120.61	120.46	120.43	120.49	120.46
C2-C3-C4	120.22	120.16	120.11	120.16	120.17	120.15	120.16	121.10	120.73	120.99	120.96	120.99	120.97
C3-C4-C5	119.58	119.73	119.73	119.67	119.67	119.66	119.66	118.52	118.91	118.71	118.76	118.67	118.72
C2-C1-C6	119.00	119.29	119.16	118.93	118.98	118.92	118.95	118.53	118.41	118.38	118.45	118.37	118.42
C2-C1-N	118.45	117.74	117.88	117.93	117.93	118.16	118.16	120.73	120.79	120.80	120.77	120.81	120.79
C-N-H13	111.24	109.66	109.09	109.08	109.12	109.99	109.94	120.95	120.85	121.00	121.06	120.96	121.01
H-N-H	107.64	105.93	106.02	104.92	104.74	106.06	105.82	118.09	118.30	117.99	117.88	118.07	117.98
ε (*tilt* angle)	1.92	2.50	2.41	2.48	2.45	2.25	2.24	0.0	0.0	0.0	0.0	0.0	0.0
ω (inversion)	52.15	56.04	57.06	57.56	57.56	55.36	55.57	0.0	0.0	0.0	0.0	0.0	0.0
C3-C2-C1-N	179.98	−179.93	−179.93	179.97	179.95	179.98	−179.97	180.0[a]	180.0[a]	180.0[a]	180.0[a]	180.0[a]	180.0[a]
C2-C1-N-H14	−120.01	−122.04	−122.30	−122.97	−123.05	−121.77	−121.95	0.0[a]	0.0[a]	0.0[a]	0.0[a]	0.0[a]	0.0[a]
Total energy (A.U.) (HF)	−285.7413	−285.7228	−285.7922	−287.5989	−287.4735	−288.5088	−287.6073	−285.7455	−285.7962	−287.6075	−287.4815	−288.5169	−287.6149
Barrier height[b] (HF)	16.491	15.992	15.861	26.655	25.705	25.065	24.013	5.380	5.403	4.165	4.645	3.649	4.213
(KJ/mol) (MP2)		18.353	17.519						9.946				

[a] Frozen.

[b] 1 KJ/mol = 83.69 cm^{-1}.

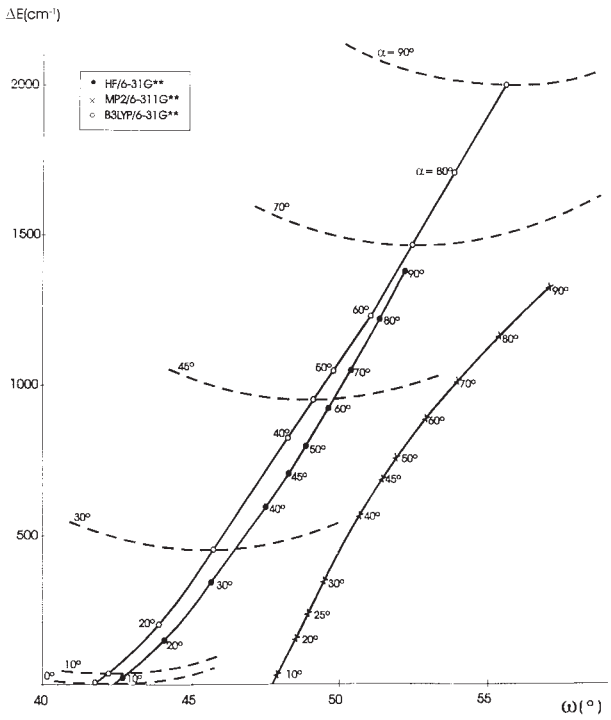

(a)

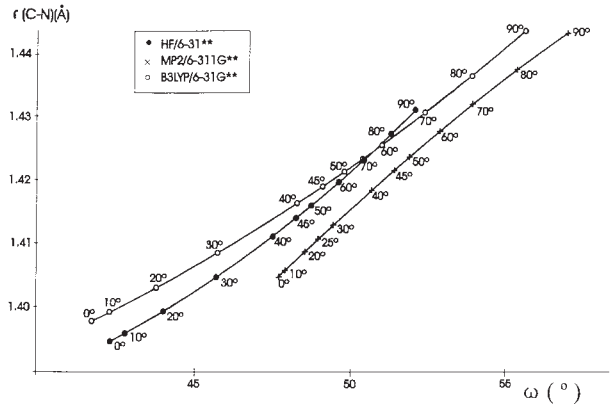

(b)

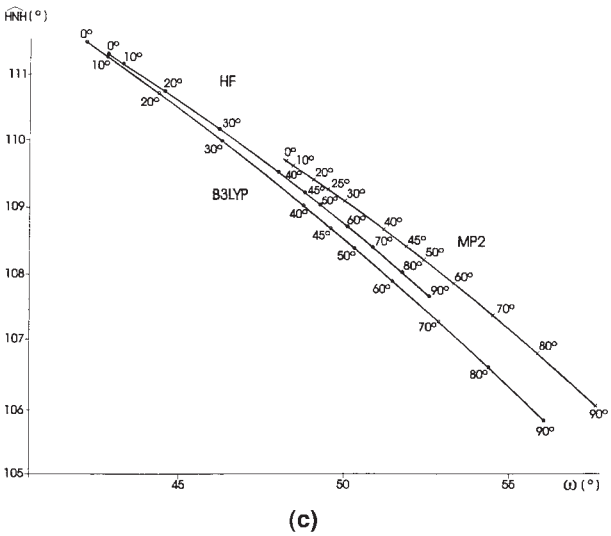

(c)

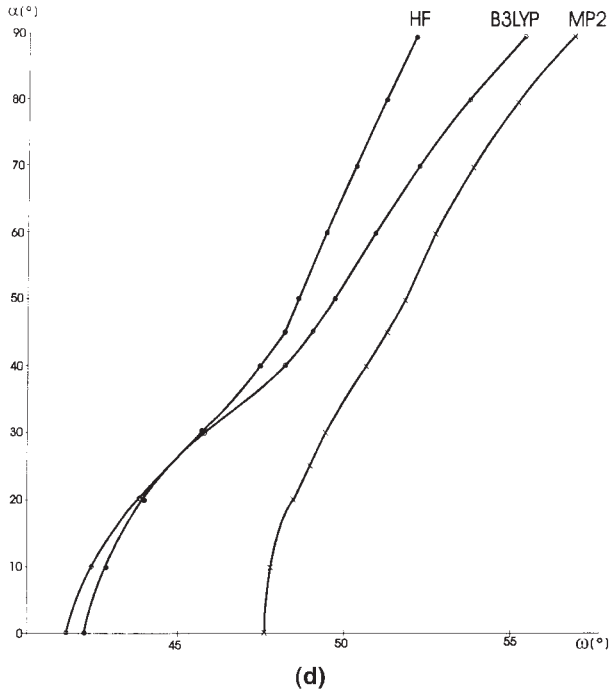

(d)

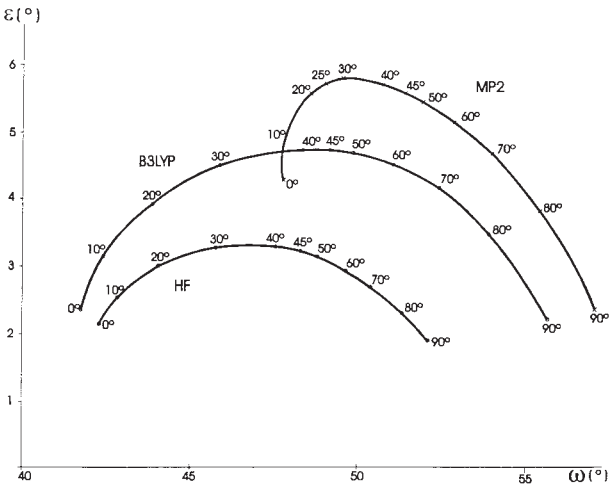

(e)

FIGURE 3. a: Energy curves for different values of the torsional angles, α, around the C–N bond and corresponding optimum inversion angles ω obtained with HF, MP2, and B3LYP procedures. b: Variation of the C–N bond and the inversion angle ω, with the torsion (α) around the C–N bond, as calculated by HF, MP2, and B3LYP methods. c: Optimum HNH and ω angles with the torsional angle α. d: Optimum inversion angles ω calculated by HF, MP2, and B3LYP in a torsion of 90°. e: Optimum inversion ω and *tilt* ε angles calculated in a torsion of 90°.

TABLE IV

Optimum values of the amino group obtained for some of the several torsional angles (α), with HF/6-31G, MP2/6-311G**, and B3LYP/6-31G** methods.**

	HF			MP2			B3LYP		
Parameters	α = 30°	45°	60°	30°	45°	60°	30°	45°	60°
C-N	1.4049	1.4144	1.4234	1.4130	1.4219	1.4320	1.4087	1.4193	1.4311
H-N-H	110.18	109.22	108.37	109.09	108.39	107.36	110.00	108.67	107.27
ε	3.27	3.21	2.72	5.80	5.57	4.71	4.48	4.73	4.20
ω	45.69	48.30	50.42	49.50	51.43	53.96	45.76	49.10	52.37
ΔE	4.113	8.33	12.464	4.155	8.23	12.197	5.432	11.38	17.500

Bond lengths in Å, angles in degrees, and increment of energy in KJ/mol.

change of the ω and ε angles (Fig. 3c), together with the $\angle$HNH, r(C–N), and r(N–H) parameters. The form of these last curves differs from that roughly obtained at the AM1 level [7]. In Figure 3e it is noted that a maximum optimum *tilt* angle appears for torsional angles around 30–45°.

Changes in the amino group structure on rotation and inversion are also quite marked, with alterations in N–H bonds and CNH angles, all showing the most stable pyramidal form to be intermediate spacing between the planar (most conjugated) and the rotated (least conjugated) conformations. The angle changes are so great as to correspond to nearly pure sp^2 hybridization in the completely planar case and essentially sp^3 hybridization in the rotated pyramidal form [2].

CHARACTERIZATION OF THE RING NORMAL MODES

The ring vibrational modes characterized at the B3P86/6-31G** level in aniline molecule are plotted in Figure 4. The motions are represented when the vector corresponding to the atomic displacement for each atom and computed frequency is $\geq$0.07 for the carbon and nitrogen atoms, and $\geq$0.15 for the hydrogen atoms. The dark arrows and circles indicate large displacements. In the literature [44], the ring modes appear characterized by the direction of the displacement vector, but in the present work they are also identified by their values. In the following paragraphs the values of this displacement are expressed in parentheses. The identification and description of the different modes by the various methods used are established with respect to Figure 4, which is selected as a reference system because their scaled results, as with B3LYP, are the nearest to the experimental data, and are as follows.

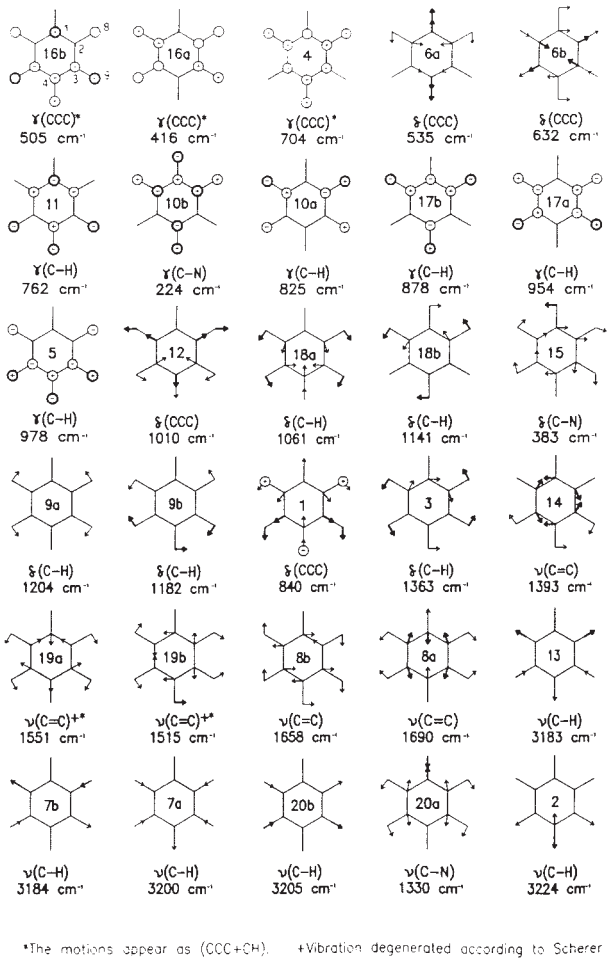

FIGURE 4. Characterization of the ring modes by the Cartesian displacements and frequencies as calculated in aniline molecules at the B3P86/6-31G** level. The orientation of the molecule corresponds to that plotted in Figure 1.

The calculated wavenumbers are shown in Table V. The normal modes (first column) are labeled according to the convention used by Varsànyi [44] for substituted benzenes, adapted from the Wilson notation for benzene [45]. The discrepancies observed in the characterization of the ring modes with other methods are plotted in Figure 5. It is important to describe well all the modes by different methods, especially the semiempirical, for the assignments when they are used in large systems derivatives of aniline.

Modes With the Same Characterization by All Theoretical Methods

Modes 6, 7b, 10b, 16a, 19b, and 20b show the same direction and in general similar values of the displacement vector by all the theoretical methods. However, this fact is not associated with a similar calculated wavenumber, the methods differing greatly, ~150 cm^{-1} in 19b and ~500 cm^{-1} in 7b and 20b.

In modes 7b and 20b the displacements of the entire C are very short (0.03–0.04); thus, they are not plotted in Figure 4, although they appear in the literature [44]. In the description by AM1 and SAM1 of mode 7b, the displacement of H9 is about twice H8, but with PM3 and ab initio methods it is half. The opposite occurs with mode 20b. In mode 19b the displacement of the C with the semiempirical is almost twice that of ab initio (~0.13), while the displacement of H9 and H10 are slightly lower. Modes 6a and 6b represent bending of the C and H atoms, which appear more deformed than as defined in the literature [44], in exactly a straight line toward the C–H bond. This was also observed in the benzene molecule [22]. The C–N out-of-plane bending vibration γ(C–N) is related to the mode 10b of benzene, in accordance with Varsànyi [44].

It is noted that with a simple monosubstitution of the benzene ring, the values of the displacement vector with the different methods change drastically, and thus the modes determined in the benzene molecule [22] with similar characterization by all the methods are very different from those in aniline.

Modes With Differences in Characterization by Theoretical Methods

Tangential Vibrations. In the characterization of modes 8a and 8b by our theoretical methods, remarkable differences appear from its definition in the classical literature [44]. Thus, the hydrogen atoms move in an opposite direction to the carbon atoms, when in the literature they appear to move in the same direction. In 8a the values of the displacement of the H differs from the various methods, and in some cases are too small to be represented, as can be seen in Figure 5a.

Modes 8a and $\beta_s(NH_2)$ are strongly coupled and appear calculated differently by the distinct methods. Thus, by AM1, PM3, SAM1, SVWN, and SLYP, modes 8a and 8b, are calculated at higher wavenumber than β_s. In contrast, by MNDO, HF, MP2, and BLYP, the mode β_s is calculated at higher wavenumber than 8a and 8b. By BP86, B3LYP, B3P86, and B3PW91, this fact depends on the basis set used; e.g., with 6-31G* or 6-311G(2d,p), β_s is determined at a higher wavenumber than 8a and 8b, while with 6-31G**, β_s is identified at a higher wavenumber than 8b but at lower than 8a. This is a consequence of the strong coupling between 8a and β_s with a small difference in the displacement vector of both modes, which can lead to a mislay in the assignment of these modes. The fact is that with all the methods (except MNDO) the mode that appears at higher wavenumber (8a or β_s) has a remarkably higher calculated intensity, contributing to the mistake. Mode 8b does not offer these problems and can be clearly identified, although it is coupled with $r(NH_2)$ instead of with $\beta_s(NH_2)$, as mode 8a.

The C and H of the C–H bonds of mode 14 are described by all the semiempirical methods with the same direction of displacement vector. However by the HF, MP2, and DFT methods they appear in the opposite direction (Fig. 5a), and in contrast to that reported in the literature [44]. This feature was observed and discussed in the benzene molecule [22]. Remarkable differences in the value of the displacement vector are obtained with the theoretical methods used, and in some cases they are too small to be plotted, as can be seen in Figure 5a.

In aniline, as monosubstituted benzene, mode 15 is a C–N in-plane bending vibration. It corresponds to an in-plane rotation in one way of the amino group and a rotation in the opposite way of the phenyl group. This description is therefore completely different from benzene.

In mode 19a the direction of the displacement of the H is opposite to the C, while in mode 18a it is in the same direction. But both cases are in contrast to that reported in the literature [44], in which they are in the same direction (mode 19a), or in the opposite (mode 18a). This fact was discussed regarding benzene [22]. Differences in the values of the displacement vector are obtained with the semiempirical

TABLE V

Calculated frequencies (in cm^{-1}) and intensities by semiempirical, ab initio, and density functional methods in aniline molecule.

Ring mode	AM1		PM3		SAM1		HF/6-31G**			MP2/6-31G*		SVWN/ 6-31G**	
Wilson no.	Freq.	Int.[a]	Freq.	Int.[a]	Freq.	Int.[a]	Freq.	Int.[a]	Activ.[b]	Freq.	Int.[a]	Freq.	Int.[a]
1	1201	0	1125	2	1169	2	890	3	7	845	4	830	1
2	3204	17	3081	13	2906	7	3371	7	100	3249	4	3146	2
3	1334	2	1239	0	1211	0	1488[d]	0	0	1385[d]	0	1301[d]	0
4	630[e]	100	635	10	590[h]	16	772	3	4	456	2	684	6
5	999	2	1012[e]	29	863	0	1108	0	0	880	1	936	0
6a[g]	565	14	537	0	544	4	574	1	2	538	1	524	1
6b	658	0	630	0	632	0	681	0	2	636	0	616	0
7a	3192	6	3063	5	2885	17	3347	3	63	3227	0	3122	0
7b	3182	1	3052	4	2866	3	3332	1	47	3210	1	3102	1
8a	1784[g]	45	1791[g]	27	1763	100	1798[g]	3	4	1689[g]	7	1672[g]	45
8b[d]	1751	3	1776	1	1726	0	1788	4	2	1670	0	1631	2
9a	1252	0	1169	0	1163	7	1293	3	2	1232	1	1160	2
9b	1198	1	1158	0	1134	1	1249[d]	1	4	1213	0	1138	0
10a	878	0	839	0	911	0	926	0	2	799	0	790	0
10b	201	1	196	2	210	0	246	2	1	218	1	217	2
11	807	59	766	34	773	2	845	36	1	708	27	737	15
12	943	3	866	13	920	2	1083	0	10	1025	0	984	0
13	3182	4	3052	3	2862	4	3329	6	4	3209	4	3102	5
14	1398	11	1327	11	1385[d]	54	1356	2	0	1474	2	1427	3
15[d]	448	0	412	0	418	1	412	0	0	382	0	372	0
16a	372	0	358	0	382	0	457	0	0	398	0	406	0
16b[e]	490	12	467	7	502[e]	39	554	22	0	510	7	510	7
17a	980	0	970	0	853	0	1088	0	0	871	0	907	0
17b	930	7	909	14	854	0	990	6	1	819	0	841	3
18a	1109	0	1049	2	1066	3	1128	1	5	1070	1	1042	1
18b	1226[d]	0	1116[d]	0	1121	3	1191	6	0	1099[d]	1	1099[d]	2
19a	1666[g]	44	1580[g]	54	1596[g]	17	1668	24	0	1565	17	1520[g]	13
19b	1588	3	1553	5	1560	21	1634	1	0	1530	1	1481	0
20a[f]	1486	1	1369	13	1452	55	1394	20	4	1329	11	1327	8
20b	3191	38	3068	29	2887	39	3353	19	7	3232	8	3126	6

[a] Relative infrared intensity, %; [b] Relative Raman intensity, %; [c] From Ref. 15; [d] $+r(NH_2)$; [e] $+W(NH_2)$; [f] As ν(C-N)$+\beta_s(NH_2)$; [g] $+\beta_s(NH_2)$; [h] $+\gamma$(C-N); [i] Far-IR of Ref. 18.

* Experimental frequency selected.

methods, because they appear strongly coupled with the scissor deformation $\beta_s(NH_2)$. Vibrations 19a,b are very strongly coupled with the vibrational pair 18, in agreement with Scherer [46].

Radial Vibrations. The motion of the ring-breathing mode 1 is not exactly in a radial direction, differing remarkably from those of the benzene molecule. In addition, this mode 1 is characterized by the ab initio methods as a mixing of in-plane and out-of-plane vibrations, in contrast to its definition in the literature [44]. This fact makes the identification of this mode difficult, and leads, in the semiempirical methods, to remarkably large errors in its calculated wavenumber, and a bad transferability of the scaling procedures.

Similarly, in mode 12 the directions of some of the atomic motions are not in a radial direction, as in mode 1. In addition to its bad characterization by AM1 and PM3, this mode is mixed with out-of-plane motions, which leads to large errors, especially in the scaled wavenumbers. It is also noted that in the case of semiempirical methods the assignment of modes

BP86/ 6-31G**	BLYP/6-31G**		B3P86/ 6-31G**		B3LYP/6-311G (2d,p)		B3PW91/ 6-31G**	Infrared[c]		Raman[c] Liquid	
Freq.	Freq.	Int.[a]	Freq.	Int.[a]	Freq.	Int.[a]	Freq.	Vapor	Solution	Freq.	Act.[b]
812	809	1	840[g]	1	833.2	1	837	812 vw*	808	812	47
3129	3123	7	3224	5	3187.6	5	3220	—	3074*	3072	28
1319[d]	1332[d]	0	1363[d]	0	1375.8[d]	0	1363[d]	—	1340*	—	
678	681	2	704	5	704.9	9	704	690 s*	689	690	1
932	937	0	978	0	968.6	0	978	—	968 w*	970	5
519	521	2	535	2	538.8	2	534	—	526 w*	533	11
613	618	0	632	0	638.6	0	631	—	619 vw*	621	11
3105	3100	1	3200	1	3164.6	1	3196	3056*, 3050	3050 sh	3053	38
3088	3084	2	3184	2	3148.6	2	3180	3025 m*	3013	3010	3
1627[g]	1602[g]	11	1690[g]	54	1646.9[g]	8	1687[g]	—	1603 vs*	1602	92
1590	1579	1	1658	2	1628.5	2	1653	—	1590 sh*	—	
1170	1175	3	1204	3	1202.1	3	1205	1180, 1173*, 1166	1173 s	1176	10
1149	1157	0	1182	1	1180.9	1	1182	—	1152 m*	1155	20
790	796	0	825	0	821.1	0	825	830, 820 vw*	823	825	47
215	216	2	224	2	221.7	2	223[h]	216.5*[i]	—	233	10
730	735	20	762	26	764.0	26	761	760, 753, 745 s*, 740	747	755	8
978	981	0	1010	0	1015.7	1	1008	983, 996*, 990 m	996	998	100
3087	3083	7	3183	7	3147.7	7	3179	3046 s*, 3036	3040	3040	15
1365[d]	1340	2	1393[d]	3	1341.5[d]	3	1388[d]	—	1324 w*	—	
371	373	0	383	0	383.7	0	383	392, 388*	390 m	390	8
401	404	0	416	0	418.8	0	416	—	—	415*	3
489[e]	492	17	505	32	507.9	18	505	500 m*	501	—	
906	910	0	954	0	947.8	0	954	—	957 w*	—	
836	842	3	878	4	879.3	4	878	874 s*	874	—	
1026	1022	1	1061	1	1048.8	1	1059	1028 m*	1028	1029	53
1109[d]	1113[d]	1	1141[d]	2	1140.1[d]	1	1141[d]	1090 m*, 1084, 1077	1115	1120	2
1498	1497	15	1551[g]	23	1537.5	21	1549[g]	1510, 1503 vs*, 1496	1501	1501	6
1465[d]	1467	0	1515[d]	1	1507.8	1	1513	—	1470*	1468	3
1285	1272	19	1330	18	1300.0	19	1326	1283, 1276*, 1270	1278	1279	25
3110	3105	18	3205	14	3170.0	14	3201	3094, 3084*	3094 w	—	

12 and 1 are in inverse order of wavenumbers with respect to the experimental data.

Mode 20a is a stretching C–N mode with contributions from CCC stretching and C–H bendings and with the direction of the motion of the C and H atoms resembling 8a. It is also coupled with β_s (NH_2). Mode 2 mainly corresponds to a stretching of the C4–H10 bond, while mode 13 is referred to C2–H8 and C6–H12 bonds.

In modes 7a and 13 the displacements of the C are very small (between 0.01–0.05) with all the methods, and are not shown in Figure 4. Mode 3, corresponding to a rotation of ring H in one direction and of C in the opposite involves r(NH_2), except with the semiempirical methods. Differences in the value of the displacement vector of the C atoms are observed by the distinct methods.

Modes 9a and 18a appear unchanged from benzene, and thus they can be clearly identified in aniline, except by SAM1, with remarkable differences (Fig. 5b). Mode 9b refers mainly to C4–H10 especially with the semiempirical methods, and partially to C3–H9 and C5–H11 bonds, differing from the characterization given by Varsànyi [44] for monosubstituted benzene. Mode 18b is difficult to assign, because it results from complicated mixings with the r(NH_2) mode, which differs depending on the ab initio or semiempirical method used. It leads

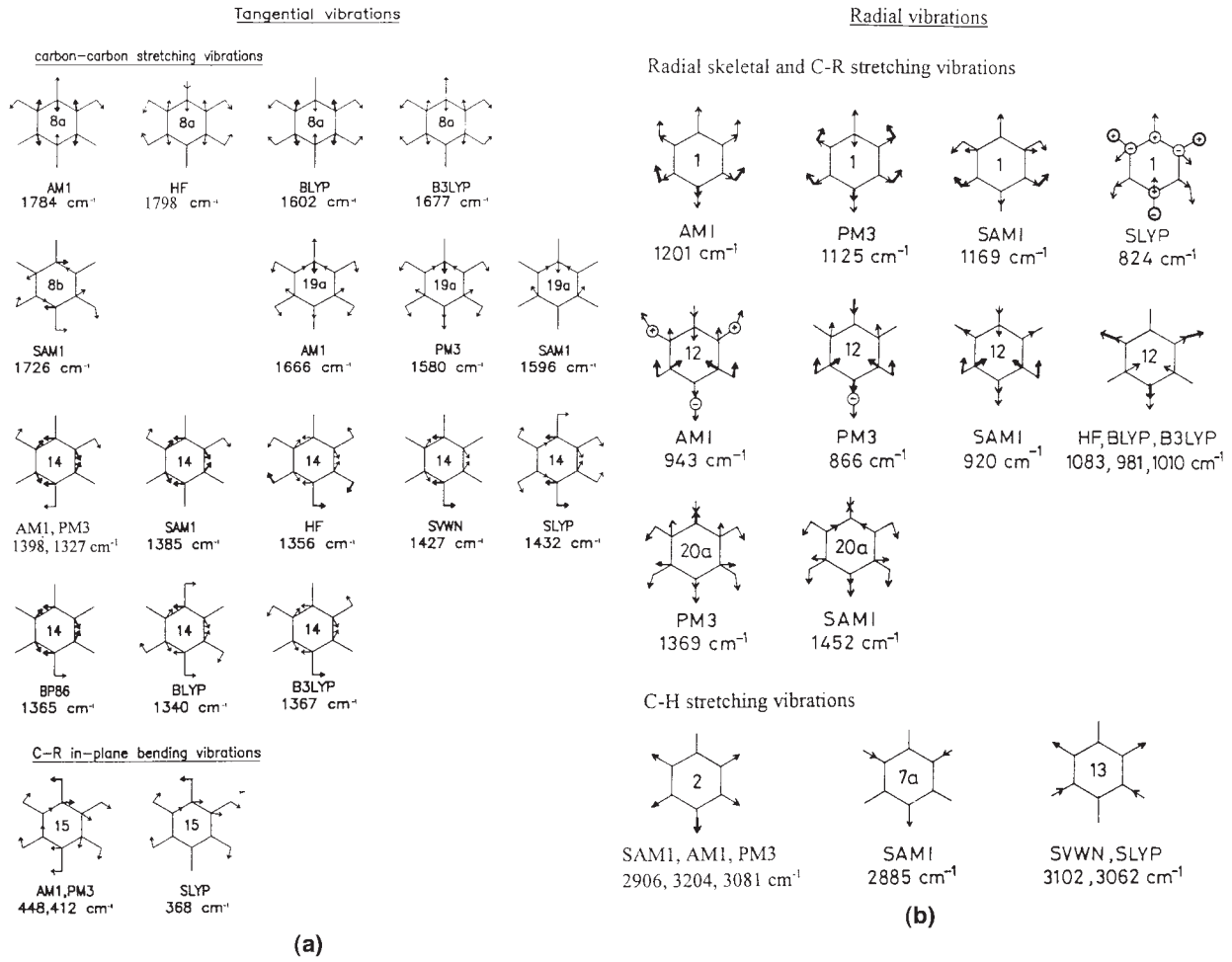

FIGURE 5. Specific characterization of several ring modes by the theoretical methods, with their respective calculated frequencies. a: Tangential vibrations. b: Radial vibrations. c: Out-of-plane vibrations.

to mislaying with mode 9b, especially if last one is calculated at a lower frequency than 18b, e.g., by AM1 in Ref. 6. Differences in the direction and in the values of the displacement vector can be observed between both modes, 9b and 18b, and they are not so close as to be confused with mode 15, as reported by Castellá-Ventura and Kassab [6].

Out-of-plane Vibrations. Modes 4 and 5 are badly characterized by MP2, which leads to a very great error in their calculated and scaled wavenumbers, which is only reduced with specific scale factors. This fact was observed and explained in benzene [22]. Remarkable differences in the values of the displacement vector appear with the semiempirical methods (Fig. 5c). By AM1, mode 4 slightly involves a δ(CCC) deformation, also implied in mode 6a.

In addition to modes 4 and 5, SAM1 also differs in the description from the other out-of-planes modes, 10a, 11, 16b, 17a, and 17b. This fact leads to a poor prediction and scaling of their wavenumbers, SAM1 being the worst of the methods used. Similarly, MP2 also differs in the description of modes 11, 16b, 17a, and 17b. Only by SLYP does mode 17b appear strongly coupled with mode 1.

WAVENUMBER CALCULATIONS

The crucial problem for wavenumber calculations with quantum chemical methods, both by semiempirical and ab initio methods, is to account for errors which result from deficiencies of the quantum mechanical methods and from the harmonic approximation [21]. These errors can be partially corrected by scaling procedures. For this pur-

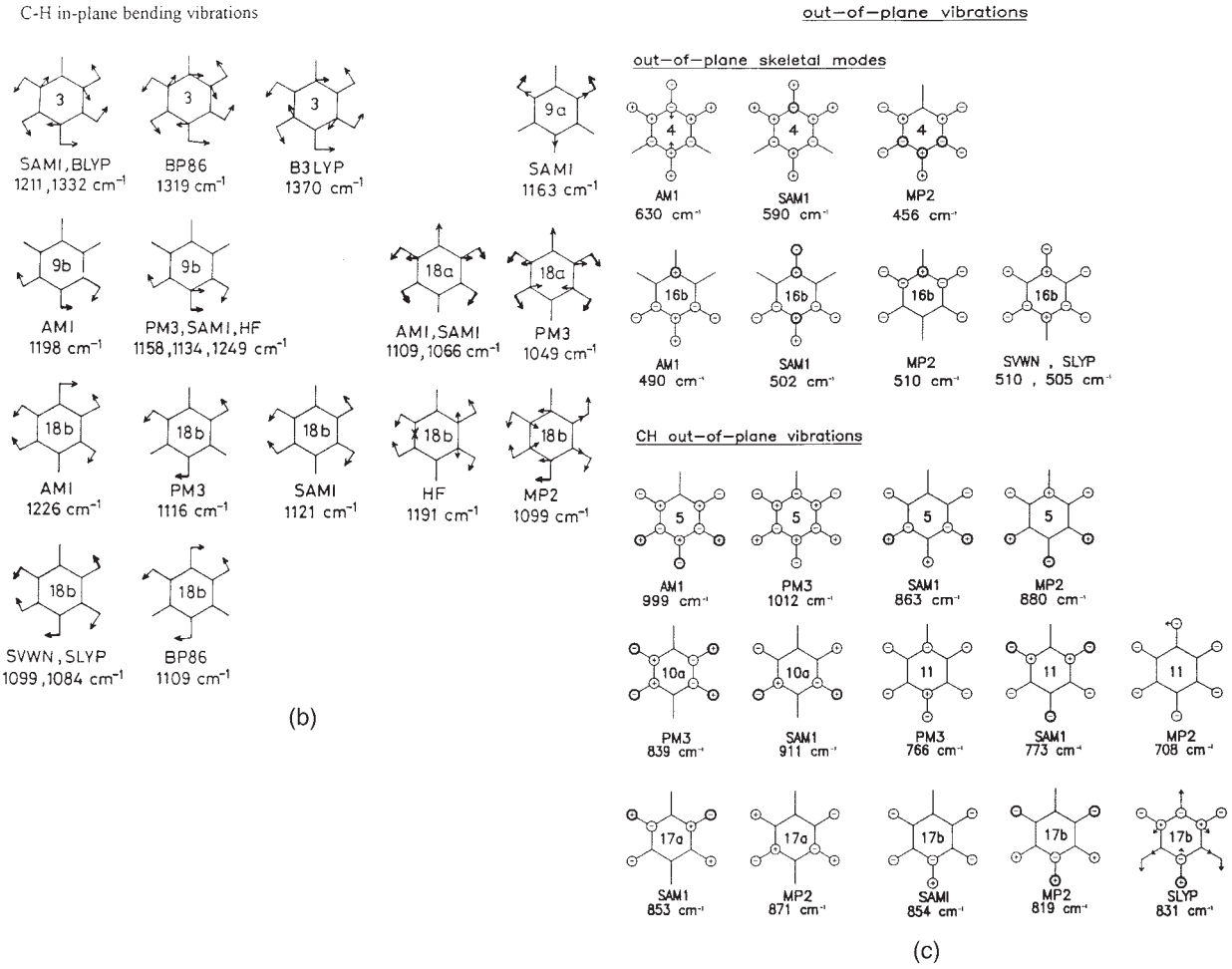

FIGURE 5. Continued.

pose, the study was divided into two sections, the phenyl-ring modes and the amino group modes.

NORMAL RING VIBRATIONS

Table V collects the theoretical and experimental wavenumbers, with their respective intensities, determined in the ring modes of aniline molecules. The last four columns show the infrared and Raman wavenumbers as reported by Evans [15] in the vapor, solution, and liquid state, together with their respective IR and Raman intensities. Asterisks mark the wavenumbers selected as representative of the modes and thus to be compared with the theoretical. For this selection, bands in vapor phase and with strong intensity were preferred. Although Niu et al. [3] and Rauhut and Pulay [19] did not use the Wilson numbers [44, 45] to assign the ring modes, we have deduced them from their calculated wavenumbers, and thus the discussion below is on this basis.

Several discrepancies in the assignment were observed. Thus, we have reversed Evans' assignment for the band at 1340 cm^{-1}, a C–H band (mode 3) instead of a combinational band given by Evans [15]. Our assignment is in agreement with the analysis of Rauhut and Pulay [19], and in contrast to Niu et al. [3]. Another discrepancy is in the ring stretching (mode 14), related by Rauhut and Pulay to the experimental band at 1308 cm^{-1}, but associated by us with the band at 1324 cm^{-1} in agreement with Evans. The band at 1324 cm^{-1} is slightly more intense than at 1308 cm^{-1}, and thus was selected. Niu et al. [3], however, did not characterize theoretically any ring stretching in this region, and mode 14 corresponds to the scaled wavenumber at

1212 cm^{-1} and erroneously related to an IR band at 1190 cm^{-1}, perhaps by the use of a small basis set, and thus failed in the assignment, as pointed out later by Rauhut and Pulay [19]. Castellá-Ventura and Kassab [6] accepted the Evans assignments but Song et al. [47] related the Evans band at 1324cm^{-1} to mode 3 and the band at 1468 cm^{-1} to mode 14, clearly inconsistent. Also, the theoretical characterization of the C–H stretches by Song et al. [47] are inconsistent with the Varsànyi definition of the modes [44], and also with our results and those of Castellá-Ventura and Kassab [6].

The identification of mode 20a as a ν(C–N) mode is in accordance with Castellá-Ventura and Kassab [6], but it is in disagreement with Song et al. [48] and Chernoff and Rice [38], and with the usual ideas according to which in monosubstituted benzenes, with a "light" substituent X, the C–X stretching is derived from the vibrational mode 7a or 13 of benzene [44].

Mode 2, predicted with the highest Raman intensity, was related to the medium Raman band at 3072 cm^{-1} (3074 cm^{-1} in IR) instead of the IR bands at 3084 and 3094 cm^{-1} (mode 20b), depolarized in Raman. This assignment is in agreement with Castellá-Ventura and Kassab [6] and consistent with the results of Rauhut and Pulay [19], but contradict the Varsànyi [44] identification of mode 2 at the highest wavenumber of the C–H stretching ring modes. However, certain uncertainties appear about mode 20b, related by several authors [3, 6, 19, 47] to the weak IR band at 3089 cm^{-1}(average of 3094 and 3084 cm^{-1}) but calculated theoretically with medium-strong IR intensity and higher than the other C–H stretches. Also, this assignment contradicts Varsànyi [44], where mode 20b corresponds to the band at 3037 cm^{-1}.

Uncertainties also appear with the selection of the wavenumber for mode 18b. In IR a band with three peaks at 1090, 1084, and 1077 cm^{-1} appears in vapor phase, which change to a unique band (~30 cm^{-1} shifted) at 1115 cm^{-1} in solution or 1120 cm^{-1} in liquid state (Raman). Rauhut and Pulay [19] selected the wavenumber at 1115 cm^{-1}, Varsànyi [44] and Castellá-Ventura and Kassab [6] that at 1084 cm^{-1}, and Niu et al. [3] at 1090 cm^{-1}. We preferred the latter, intermediate between the other two options.

Mode 10b has been related [3, 6, 19, 44] to the Raman band at 233 cm^{-1}; however, according to our calculations, and also with the theoretical results of Rauhut and Pulay [19] and Niu et al. [3], it corresponds to the far-IR band that has been observed in the spectra [18] at 216.5 cm^{-1} and considered by Song et al. [47].

We reversed the assignments of modes 10a and 11 given by Evans [15]; indeed, we calculated the A″ wavenumber higher than the A′ wavenumber, independent of the method used. Our assignment disagrees with Seeger et al. [48], but it is in agreement with the results of Niu et al. [3], Castellá-Ventura and Kassab [6], and Varsànyi [44].

A discrepancy with Varsànyi is observed in mode 7a assigned to the Raman band at 3010 cm^{-1}, while by other authors [3, 6, 19, 47] it corresponds to mode 7b.

In addition to the discrepancies mentioned above for modes 14 and 20a, Ref. 47 also fails in the theoretical identification and/or experimental correspondence in modes 1, 4, 8, 9b, 12, 16, 18b, and 19, in general based on the Chernoff and Rice [38] assignment but in contrast to our results and other authors [3, 6, 19, 44]. Thus, it will not be considered further. Similarly, the work of Seeger et al. [48], having numerous discrepancies with our results and with those of other authors [3, 6, 19, 44], will not be considered here.

The difference between the calculated and experimental wavenumbers, $\Delta(\omega^{cal} - \nu^{exp})$, are listed in Table VI. The largest absolute errors are in bold. The bottom row shows the root-mean-square error (rms) obtained with the different methods. Their values are in agreement with those determined for benzene [22].

In the C–H stretching region, modes 2, 7, 13, and 20b appear, in general, strongly overestimated (by SAM1 underestimated) by all the methods, except by PM3, with accurate predictions. In the medium and low region the error in modes 1, 3, 4, and 5 differs remarkably depending on the method used, but in modes 6a, 6b, 15, 16a, and 16b it is slight.

In the semiempirical methods it is noted in general that AM1 overestimates the wavenumbers, while SAM1 underestimates the values. Although it is the newest semiempirical method, SAM1 shows greater errors than AM1 and PM3. PM3 gives the best-calculated wavenumber in the C–H region (even better than HF, MP2, and DFT methods) with a very low error, around 10–15 cm^{-1}, although it fails dramatically in the prediction of modes 1, 8a, 8b, and 12. MNDO is the oldest of the four semiempirical methods used, and consequently the calculated wavenumbers, not shown in the table, are the poorest.

In Hartree-Fock, all the wavenumbers are overestimated and in agreement with the 10–20% of

TABLE VI

Absolute errors ($\Delta\nu = \omega^{\text{calculated}} - \nu^{\text{experimental}}$) determined for the normal ring modes of the aniline molecule.

Ring mode Wilson no.	Semiempirical			Ab initio			DFT methods							
	AM1	PM3	SAM1	HF/ 6-31G**	HF/6-31++G**	MP2/ 6-31G*	SVWN/ 6-31G**	SLYP/ 6-31G**	BP86/ 6-31G**	BLYP/ 6-31G**	B3P86/ 6-31G**	B3LYP/ 6-31G**	B3LYP/ 6-311G (2d,p)	B3PW91/ 6-31G**
1	**389**	**313**	**357**	78	74	33	18	12	0	−3	28	23	21.2	25
2	130	7	−168	**297**	**299**	175	72	35	55	49	150	133	113.6	146
3	−6	−101	−129	148	146	45	−39	−62	−21	−8	23	30	35.8	23
4	−60	−55	−100	82	78	**−234**	−6	−12	−12	−9	14	15	14.9	14
5	31	44	−105	140	148	−88	−32	−47	−36	−31	10	10	0.6	10
6a	39	11	18	48	46	12	−2	−7	−7	−5	9	10	12.8	8
6b	39	11	13	62	60	17	−3	−10	−6	−1	13	16	19.6	12
7a	137	7	−171	**291**	**293**	171	66	28	49	44	144	128	108.6	140
7b	157	27	−159	**307**	**309**	**185**	77	37	63	59	159	143	123.6	155
8a	**181**	**188**	160	**195**	**187**	86	69	67	24	−1	87	74	43.9	84
8b	161	**186**	136	**198**	**188**	80	41	38	0	−11	68	53	38.5	63
9a	79	−4	−10	120	117	59	−13	−32	−3	2	31	31	29.1	32
9b	46	6	−18	97	93	61	−14	−33	−3	5	30	32	28.9	30
10a	58	19	91	106	104	−21	−30	−41	−30	−24	5	7	1.1	5
10b	−16	−21	−7	29	26	1	0	−2	−2	−1	7	7	5.2	6
11	62	21	28	100	98	−37	−8	−16	−15	−10	17	18	19.0	16
12	−53	−130	−76	87	77	29	−12	−19	−18	−15	14	14	19.7	12
13	136	6	**−184**	**283**	**286**	163	56	16	41	37	137	121	101.7	133
14	74	3	61	32	31	150	103	108	41	16	69	43	17.5	64
15	60	24	30	24	23	−6	−16	−20	−17	−15	−5	−4	−4.3	−5
16a	−43	−57	−33	42	42	−17	−9	−11	−14	−11	1	3	3.8	1
16b	−10	−33	2	54	52	10	10	5	−11	−8	5	7	7.9	5
17a	23	13	−104	131	138	−86	−50	−65	−51	−47	−3	−4	−9.2	−3
17b	56	35	−20	116	115	−55	−33	−43	−38	−32	4	5	5.3	4
18a	81	21	38	100	94	42	14	8	−2	−6	33	27	20.8	31
18b	57	26	31	101	101	9	9	−6	19	23	51	52	50.1	51
19a	163	77	93	165	156	62	17	5	−5	−6	48	43	34.5	46
19b	118	83	90	164	156	60	11	3	−5	−3	45	43	37.8	43
20a	**210**	93	176	118	107	53	51	45	9	−4	54	39	24.0	50
20b	107	−16	**−197**	**269**	**278**	148	42	4	26	21	121	105	86.0	117
rms	117	88	140	158	156	96	42	37	27.4	23.3	67	59	49.2	64.7

The largest absolute errors are printed in bold type.

TABLE VII

Errors obtained in the calculated and scaled frequencies of the aniline ring modes by the different procedures, methods, and levels.

	Calculated frequencies					Scaled frequencies with an overall factor				
				Largest error					Largest error	
Method	rms	MAD	SD	Positive	Negative	rms	MAD	SD	Positive	Negative
Semiempirical										
MNDO	181	140.0	115.2	377 (7b)	−125 (12)	—	—	—	—	—
AM1	117	92.7	76.9	389 (1)	−60 (4)	80	49.0	62.8	333 (1)	−89 (4)
PM3	88	54.6	68.8	313 (1)	−130 (12)	84	56.9	61.5	286 (1)	−151 (12)
SAM1	140	93.5	78.6	357 (1)	−197 (20b)	—	—	—	—	—
SCF										
HF/6-31G*	164	138.5	88.7	320 (7b)	—	30.9	21.5	22.2	25 (5)	−104 (14)
HF/6-31G**	158	132.8	83.0	307 (7b)	—	31.2	21.8	22.3	28 (5)	−105 (14)
HF/6-31++G**	156	130.7	84.6	309 (7b)	—	—	—	—	—	—
Post-SCF										
MP2/6-31G*	96	73.2	62.5	185 (7b)	−234 (4)	62	40.6	47.2	67 (14)	−212 (4)
Density functional										
SVWN/6-31G**	42	30.8	26.3	103 (14)	−50 (17a)	33	24.3	22.2	79 (14)	−66 (20b)
SLYP/6-31G**	37	27.9	24.2	108 (14)	−65 (17a)	—	—	—	—	—
BP86/6-31G**	27.4	20.8	17.9	63 (7b)	−51 (17a)	24.5	20.4	13.7	36 (7b)	−59 (17a)
BLYP/6-31G**	23.3	16.9	16.1	59 (7b)	−47 (17a)	24.3	20.6	12.7	42 (7b)	−52 (17a)
B3P86/6-31G*	69	49.0	49.1	160 (7b)	−9 (10b)	18.2	13.7	11.9	19 (7b)	−50 (17a)
B3P86/6-31G**	67	46.2	48.4	159 (7b)	−5 (15)	19.1	14.8	12.0	18 (7b)	−45 (17a)
B3LYP/6-31G*	61	43.4	42.5	145 (7b)	−10 (17a)	16.9	13.8	9.7	23 (7b)	−46 (17a)
B3LYP/6-31G**	59	41.3	41.8	143 (7b)	−4 (15,17a)	18.6	15.5	10.1	21 (7b)	−45 (10a)
B3LYP/6-311G(2d,p)	49.2	34.6	35.0	124 (7b)	−9 (17a)	—	—	—	—	—
B3PW91/6-31G**	64.7	44.5	47.0	155 (7b)	−5 (15)	18.8	14.9	11.5	19 (7b)	−44 (17a)

average error established for this method [49, 50]. This overestimation depends on the type of vibrational mode and wavenumber range, varying between 2–13% in our case. It is noted that in HF the rms error with the 6-31G** or 6-31++G** basis set is higher than that obtained with the modest semiempirical methods, which are also higher than with MP2. The inclusion of two rows of "diffuse" functions to the 6-31G** basis set leads to small changes in the wavenumbers, ~10 cm^{-1} in modes 5, 8a, 8b, 12, 19a, 19b, 20a, and 20b, and significant improvements in the IR intensities as a consequence of the slight reduction in the absolute IR intensity predicted for the W(NH_2) mode, which, as discussed below, is a failure of the theoretical methods used. This better performance of the IR intensity calculated with the 6-31++G** basis set has been observed in other molecules [51].

In MP2 the difference between the harmonic oscillator prediction and the exact or Morse potential behavior is remarkably lower, about 5% excluding mode 4. MP2 fails dramatically in the calculation of modes 2, 7a, 7b, 13, 14, and 20b, and especially in mode 4, as in benzene molecule [22]. With the increase of the basis set, the rms error is only slightly reduced.

Only with DFT methods are the wavenumbers relatively close to the experimental, BLYP being the best for this purpose. The 6-31G* or 6-31G** basis sets are the most appropriate, due to the small improvement obtained with its increase, e.g., in B3LYP/6-31G(2d,p) only a variation of 20–30 cm^{-1} was obtained in modes 2, 7a, 7b, 8a, 13, 14, and 20b. However, these results do not adequately reproduce all the experimental patterns of wavenumbers with the accuracy desired, and thus to reduce the error it is necessary to scale the wavenumbers.

SCALING THE WAVENUMBERS

The calculated wavenumbers were directly scaled by three procedures: an overall scale factor for the calculated level, a scaling equation determined at each level, and specific scale factors for

Scaled frequencies with the scaling equations					Scaled frequencies with specific scale factors				
			Largest error					Largest error	
rms	MAD	SD	Positive	Negative	rms	MAD	SD	Positive	Negative
84	50.4	67.2	300 (1)	−241 (14)	53	36.0	39.2	160 (1)	−158 (14)
81	48.8	62.5	331 (1)	−99 (12)	45	29.1	33.6	149 (20a)	−70 (12)
84	52.6	65.2	301 (1)	−140 (12)	36	23.1	26.4	100 (1)	−100 (12)
106	84.9	77.2	366 (1)	−131 (4)	58	33.5	47.9	264 (20a)	−69 (11)
23.9	16.6	17.3	39 (8a)	−87 (14)	8.5	6.0	6.0	18 (7b)	−28 (20b)
24.3	16.8	17.5	40 (8b)	−90 (14)	9.7	6.9	6.8	23 (7b)	−27 (20b)
24.3	16.7	17.7	47 (5)	−90 (14)	9.2	6.6	6.3	22 (7b)	−27 (20b)
54	38.9	38.0	99 (14)	−192 (4)	25	19.1	16.3	19 (12)	−62 (11)
28	20.2	19.1	89 (14)	−49 (3)	13	9.8	7.9	25 (8a)	−27 (20b)
33	23.5	23.7	109 (14)	−58 (3)	14	10.7	8.9	32 (20a)	−27 (20b)
17.1	13.6	10.3	40 (14)	−41 (17a)	11.8	8.8	7.9	24 (8a)	−27 (20b)
14.5	11.6	8.7	27 (18b)	−39 (17a)	11.1	8.2	7.5	28 (18b)	−26 (20b)
13.1	10.3	8.0	24 (18b)	−33 (17a)	11.1	8.0	7.6	27 (8a)	−27 (20b)
13.4	11.3	7.2	26 (8a)	−26 (17a)	10.1	7.6	6.6	20 (8a)	−27 (20b)
11.8	8.5	8.2	29 (18b)	−32 (17a)	10.8	7.7	7.6	28 (18b)	−30 (20b)
11.2	8.5	7.2	22 (18b)	−26 (17a)	12.5	9.0	8.7	37 (8a)	−27 (20b)
11.5	8.8	7.3	25 (18b)	−27 (17a)	10.7	7.7	7.4	27 (18b)	−26 (20b)
12.8	10.4	7.4	25 (8a)	−26 (17a)	10.2	7.7	6.7	20 (7b,8a)	−26 (20b)

each mode and level. The final errors are shown in Table VII.

With a Single Overall Scale Factor

The compound wavenumbers of a molecule at a specific level of theory can be scaled with a single scale factor (or correction factor), which differs for the different levels theory. This procedure is generally used in the literature to scale the calculated wavenumbers. As scale factors we used those reported by Scott and Radom [50], i.e., two scale factors, one for high and medium spectra, and the other for the low wavenumber modes, except by AM1 and PM3, with only one scale factor. Scale factors have not been reported for the MNDO, SAM1, and SLYP methods, and thus they are not included in Table VII. In the case of 6-31G** in DFT methods, scale factors with the 6-31G* basis set were used.

In general, with this procedure of scaling a remarkable reduction of the error is obtained. E.g., with B3LYP and B3P86 the drop is three times, while with AM1 and MP2 and SVWN it is about 30%. A special reduction is observed with HF, from the highest error (rms of 158 cm^{-1}) in the calculated wavenumbers of Table VI, to an rms error of 31 cm^{-1} and much better than MP2. The exceptions are the PM3 and B-bases methods, with a very low reduction of the error, or even worse, as in the case of BLYP.

With this scaling the lowest errors are obtained with the B3-exchange functional. However, its value is too high, especially in modes 5, 10a, 12, 17a, and 17b, to be used routinely. An additional reduction of the error can be reached using the next (and new) procedure of scaling.

With a Scaling Equation

From the benzene molecule, scaling equations for each level of theory were extracted [22] and used in the ring modes of the aniline molecule. The

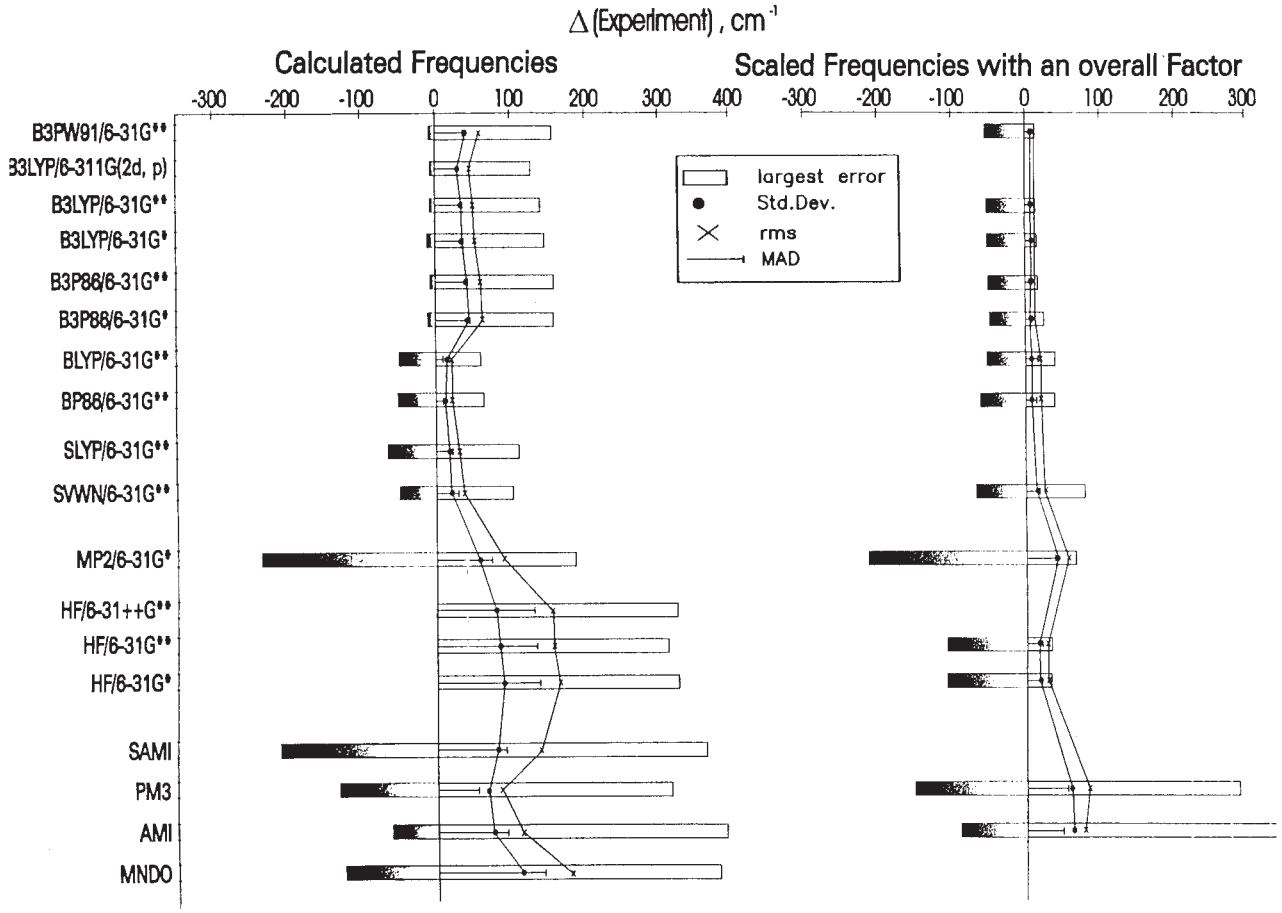

FIGURE 6. Error obtained by the different methods and levels in the calculated frequencies of the ring modes and in their scaled frequencies using an overall scale factor, a scaling equation, and specific scale factor for each mode.

final errors obtained with this procedure are also collected in Table VII.

It is noted that the scaled wavenumber of mode 12 is underestimated with all the methods, except with MP2. Its value is sensitive to the basis set, and its error is not reduced drastically until two rows of "d" functions are added, e.g., 6-311G(2d,p). Also noted is the continued great error of the sophisticated MP2 procedure. To investigate the cause, it is observed that the wavenumber of mode 4 was calculated to be far too low (~200 cm^{-1}), the poorest being determined by MP2. Its error is not significantly reduced with the use of a scale factor or a scaling equation. With the increase of the basis set the error is incremented, except when "f" basis functions are included. This fact was interpreted in benzene [22] as a lack of balance of the basis set which is almost solved with "f" basis functions. However, even with this basis set the wavenumber of mode 4 has not completely converged.

Mode 14 is a failure of MP2, SVWN, and SLYP. Scaling with a uniform scale factor remarkably reduces the error in MP2 and SVWN, although it is not further reduced with the increment of the basis set. However, this mode is poorly scaled (even increasing the error) with the scaling equations, especially with SAM1, HF, MP2, SVWN, and SLYP, and has a large error of about 100 cm^{-1}. The lack of uniformity in the description of this mode by these methods reveals the problem. Thus, we conclude that the MP2 method itself is certainly deficient for special vibrations, such as modes 4 and 14. This failure in the prediction of the wavenumbers has been observed in other molecules [52].

B3LYP procedures at 6-31G** give the best result, but its rms error is not reduced with the increase of the basis set. In general, DFT procedures with B- and B3-bases yield very low errors that are of comparable reliability. The use of the scaling equations reduces the rms errors to ~30% of those found with

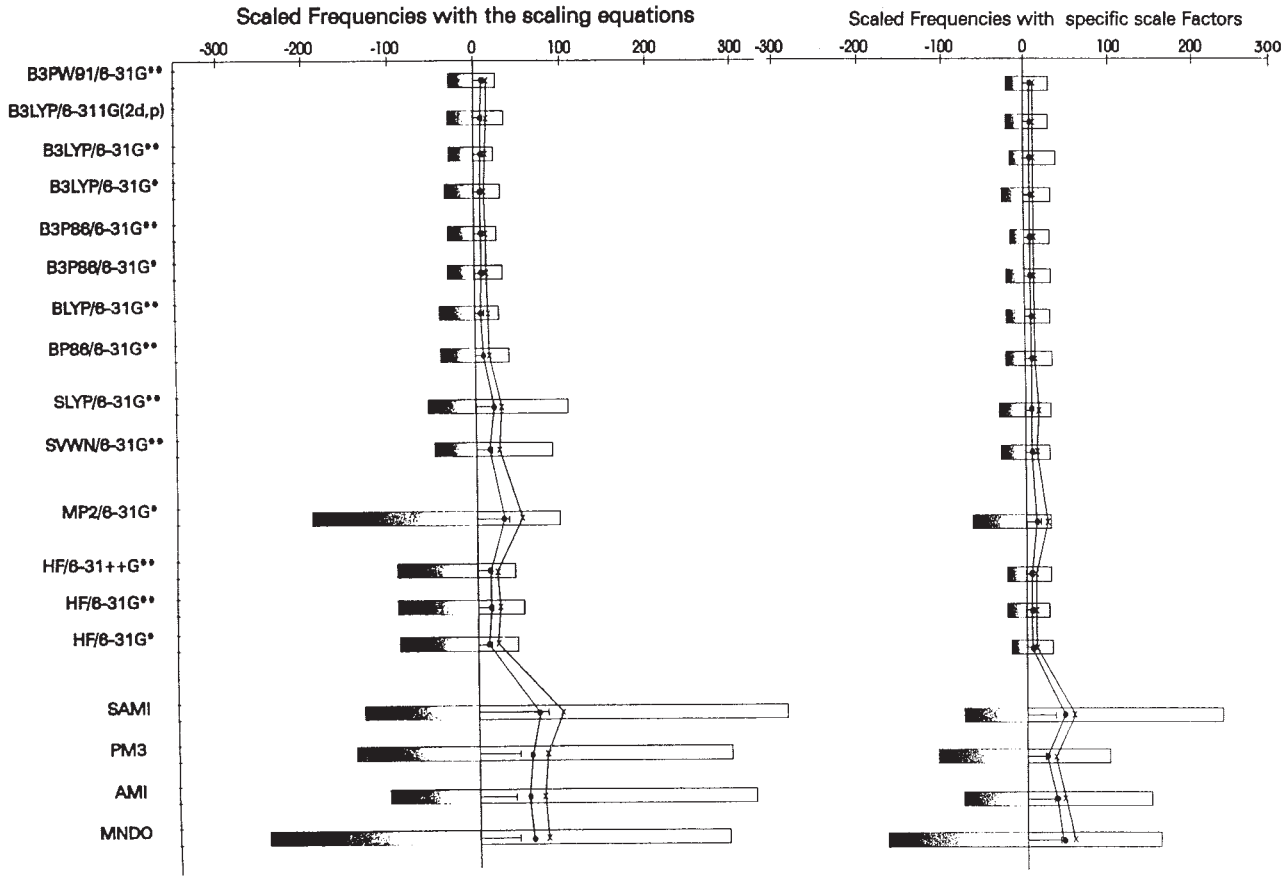

FIGURE 6. Continued.

a uniform scale factor, showing that the errors in the calculated wavenumbers with DFT methods are systematic and partially associated with the kind of molecules studied; therefore, they can reduce employing scaling equations. The exceptions are modes 8a, 10b, and 18b, in which the error is slightly increased.

With larger errors than B3LYP appear HF, SVWN, and SLYP, of comparable reliability. In them, the improvement with the scaling is ~15% over the use of an overall scale factor. The semiempirical methods (especially SAM1) and MP2 are the poorest procedures, and although with employing a scaling equation the error is remarkably reduced with SAM1 and MP2, it is still too large for these methods to be used.

With Specific Scale Factor for Each Mode

The procedure is based on the assumption that the ratios between experimental and computed wavenumbers are fairly constant for each type of characteristic wavenumber. It is thus possible to derive for a known experimental spectrum a scale factor for each characteristic wavenumber by taking the average of the ratios between the experimental and computed wavenumbers, $\lambda = \nu^{exp}/\omega^{cal}$, and to use them for predicting or assigning unknown spectra. The scale factors determined previously in the benzene molecule [22] were used to scale the wavenumbers of the ring modes of aniline. The absolute errors obtained with these procedures are collected in the last columns of Table VII. The introduction of different scale factors for distinct types of vibrational modes removes the error, which is systematic and associated with the same mode in related molecules, improving the accuracy of the methods, especially the semiempiricals, in which the error drops to about half. This procedure of scaling was tested with semiempirical methods in the ring modes of several benzene derivatives with bio-

logical and pharmacological applications [53–55], with similar errors obtained in aniline.

With HF the reduction is so high (more than half) that the scaled wavenumbers are of similar reliability, or even better than those obtained with B- and B3-bases. Although with MP2 the rms error is remarkably improved, it continues as the worst of the ab initio methods, especially because the error on modes 4 and 20b is not reduced at all, and because the error in modes 11, 13, 18b, and 20a is increased.

Thus, we recommend that in the semiempirical, HF, MP2, SVWN, and SLYP methods, with a drastic reduction of the error, the wavenumbers should be scaled with specific scale factors for each mode. Because with semiempirical methods the error is far less systematic than in HF and DFT, they should not be used except for large benzene derivatives.

Comparing these results with the absolute errors obtained in the wavenumbers by scaling the force constant matrix [3, 19], the great accuracy reached (excluding mode 14) is noted by Niu et al. [3] with the small 4-21G* basis set. Rauhut and Pulay [19] obtained a similar error to ours at the HF level, although this procedure is more complex and, as discussed earlier, the direct procedure of scaling the wavenumbers is preferable.

The results with the relative accuracies in the wavenumbers of a variety of different models is shown in graphic form in Figure 6, which plots the mean absolute deviation (MAD), the rms error, the standard deviation (SD), and the greatest positive and negative deviations from experiment for each model chemistry. The errors plotted correspond to the calculated and to the scaled wavenumbers with the three procedures of scaling described here, and for the different methods and levels under study. The numerical values obtained are given in Table VII. From these results the following is observed.

In the semiempirical methods the errors obtained in the calculated wavenumbers are in accordance with those determined in the benzene molecule [22], the best being PM3 and the worst MNDO. With the use of an overall scale factor or a scaling equation the error is reduced (very little with PM3), but this reduction may not be acceptable. Thus, specific scale factors for each mode should be used, obtaining with PM3 an MAD comparable to MP2. In MNDO and SAM1 the error is drastically reduced with the use of these specific scale factors, but continue being very large and thus are the worst methods. These results indicate that in MNDO and SAM1 the error in the calculated wavenumbers is largely inherent to the method and is not eliminated by the use of scaling procedures. However, by AM1, and especially PM3, the error is partially systematic and associated with the mode itself, with its calculated wavenumber; this error is systematic for the same mode in related molecules, and can be remarkably reduced using specific scale factors for each mode vibration. Thus, these methods should be the ones used in predicting the ring vibrations of larger benzene derivatives.

Although the semiempirical methods have better MADs than the Hartree-Fock-based methods, indicating that their parametrizations have accounted for some of the effects of electron correlation, their errors are less systematic than the HF; thus, they are less reduced with the use of scaling procedures. In HF the reduction is drastic, and although with the use of an overall scale factor, or a scaling equation, the error in several modes is still great, with the use of specific scale factors it almost disappears.

MP2 does not appear to offer a significant improvement over HF in performing the calculated wavenumbers, and in the scaled wavenumbers it shows an error more than twice as great. For this reason and because of excessive time and computer memory consumption, it is preferable to use other ab initio methods than MP2.

DFT methods are the most cost-effective procedures found for predicting the vibrational wavenumbers, and in general they can be used efficiently. Although the calculated wavenumbers by SVWN and SLYP are better than B3-bases, the scaled wavenumbers are less systematic and have the greatest error of the DFT methods, especially in modes 5, 7b, 8a, 10a, 17a, and 20, and it is not reduced enough with scaling. However, the error is generally systematic in B- and B3-bases and the use of a scaling equation or specific scale factors leads to accurate wavenumbers. The B-bases procedures, while not performing quite as well with the scaling as the corresponding B3-, have the attraction of the smallest errors in the calculated wavenumbers, and thus they can often be used without scaling.

It is noted that the wavenumber of mode 7b appears in general overestimated by all the methods, excluding PM3, SAM1, and MP2, and by the different scaling procedures; this error is not reduced even by increasing the basis set. This fact can tentatively suggest that there is a slight inexactitude in the wavenumber of the observed band.

The procedure with a scaling equation thus represents a remarkable improvement of the scaled wavenumbers over the single overall factor proce-

TABLE VIII

Calculated frequencies (in cm^{-1}) in the NH_2 group of aniline molecule with semiempirical, ab initio, and DFT methods.

	ν_{as}			ν_s			β_s (scissor)			r (rock)[f]			W (wag)[g]			τ (twist)		
	Calculated		Scaled[d]	Calculated		Scaled[d]	Calculated		Scaled[d]	Calculated		Scaled[d]	Calculated		Scaled[d]	Calculated		Scaled[d]
Methods	Freq.	Int.[a]	Freq.	Freq.	Int.[a]	Freq.	Freq.	Int.[a]	Freq.	Freq.	Int.[a]	Freq.	Freq.	Int.[a]	Freq.	Freq.	Int.[a]	Freq.
Semiempirical methods																		
MNDO	3551			3582			1830			1293			962			167		
AM1	3463	17	3301	3491	28	3328	1733	17	1652	1166	44	1111	671	86	640	265	13	253
PM3	3411	0	3329	3531	4	3447	1678	0	1638	1086	0	1060	987	100	963	229	13	224
SAM1	3514	5	—	3544	1	—	1596	17	—	1061	0	—	483	30	—	299	1	—
SCF and post-SCF methods																		
HF/4-21G*[c]		2	3483.9		9	3407.8		48	1652.6		1	1051.9		100	567.4		0	235.2
HF/6-31G	4005[b]		3586	3872[b]		3467	1842[b]		1649	1134[b]		1015	382[b]		346	344[b]		312
HF/6-31G*	3882[b]		3476	3784[b]		3388	1844[b]		1651	1155[b]		1034	719[b]		651	246[b]		223
HF/6-31G**	3911	5 (26)	3517	3804	6 (55)	3421	1821	58 (14)	1637	1146	0	1030	683	100 (3)	621	261	9 (0)	237
HF/6-31++G**	3911	6		3804	9		1816	68		1143	0		674	100		258	10	
MP2/6-31G*	3671	3	3463	3561	4	3359	1717	28	1620	1174	1	1108	746	100	782	251	8	263
Density functional methods																		
SVWN/6-31G**	3636	7	3575	3520	10	3461	1588	30	1561	1033	0	1016	448	100	452	336	5	339
SLYP/6-31G**	3588	7	—	3471	10	—	1567	39	—	1021	0	—	438	100	—	337	4	—
BP86/6-31G**	3580	3	3549	3472	3	3442	1607	2	1593	1042	1	1033	583	100	613	295	7	310
BLYP/6-31G**	3554	2	3534	3451	2	3432	1624	33	1615	1042	1	1036	596	100	633	292	7	310
B3P86/6-31G*	3681	4	3518	3578	7	3420	1701	50	1626	1083	1	1035	615	100	610	290	7	288
B3P86/6-31G**	3711	5	3547	3600	6	3441	1660	9	1587	1075	1	1027	584	100	580	297	8	295
B3LYP/6-31G*	3643.6	3	3503.0	3545.6	4	3408.7	1695.4	50	1630.0	1079.8	1	1038.1	632.4	100	633.2	285.9	8	286.3
B3LYP/6-31G**	3673	3	3531	3567	4	3429	1658	2	1594	1073	1	1032	603	100	604	292	7	292
B3LYP/6-311G(2d,p)	3636.3	4		3544.3	4		1664.0	43		1070.4	1		636.3	100		292.0	8	
B3PW91/6-31G**	3709	5	3551	3598	6	3444	1660	6	1589	1074	1	1028	585	100	581	297	7	295
Experimental[e]																		
Infrared: Vapor	3515, 3500 m[†], 3486			3418 m[†]			1628, 1619[†], 1611			—			669, 665, 658[†]			277.3[h,†]		
solution	3485			3401			1618 vs			1054[†]			570			220		
Raman: liquid	3435 (5)			3360 (15)			1620 (20)			—			650 vb			273.3		

[a] Relative infrared intensity, %. In parentheses the relative Raman activity (%).
[b] From Ref. 6.
[c] Scaling the force constant matrix [3].
[d] With the scale factors reported in Ref. 50.
[e] From Ref. 15.
[f] +18b, δ(C-H).
[g] +10b, γ(ring).
[h] Estimated [17].
[†] Frequency selected as experimental.

TABLE IX

Absolute errors determined for the calculated and scaled frequencies of the amino group modes in the aniline molecule.

	Calculated frequencies										
Mode	AM1	PM3	SAM1	HF/6-31G**	MP2/6-31G*	BP86/6-31G**	BLYP/6-31G**	B3P86/6-31G**	B3LYP/6-31G**	B3LYP/6-311G(2d,p)	B3PW91/6-31G**
ν_{as}	−37	−89	14	**411**	171	80	54	**211**	173	**136**	**209**
ν_s	73	113	126	**386**	143	54	33	182	149	**126**	180
β_s	114	59	−23	**202**	98	−12	5	41	39	45	41
r	112	32	7	92	120	−12	−12	21	19	16	20
W	13	**329**	−175	25	88	−75	−62	−74	−55	−22	−73
τ	−12	−48	22	−16	−26	18	15	20	15	15	20
rms	74	150	89	**245**	117	51	37	119	97.7	79	118

[a] From Ref. 3.
[b] From Ref. 19.

dure, about 30% in the rms error. The procedure with specific scale factor represents an improvement over the scaling equation, about 10–15% in the rms error, and should be the procedure recommended of scaling if a high accuracy in the scaled wavenumbers is required.

AMINO GROUP VIBRATIONS

In Table VIII the calculated wavenumbers for the different modes of the amino group with the distinct levels used are shown. The scaled wavenumbers using an overall scale factor are also included. At the bottom of the table is collected the experimental values reported by Evans [15].

A known error that occurs with semiempirical methods [53], and observed in our case in aniline, is that the stretching symmetric vibration appears at a higher wavenumber than the antisymmetric. By contrast, ab initio calculations are correct, the antisymmetric ν_{as} mode appearing at higher wavenumber than the symmetric. However, the computed wavenumbers by semiempirical methods are closer to the experimental than the HF, MP2, and B3-bases methods. As experimental wavenumbers, of the three bands observed in the vapor phase [15] as ν_{as}, the one at 3500 cm^{-1} has the highest intensity, and thus it was selected as representative of the mode, in agreement with other authors [3, 6, 19]. The great wavenumber shift of this mode was noted in the IR of the liquid state (3440 cm^{-1} selected by Varsànyi [44]) and in Raman (3435 cm^{-1}), far from agreement with our predictions. Regarding intensity, the calculated value of the symmetric mode in the IR spectra is slightly greater than the antisymmetric, although by SAM1 it is the opposite, and by B- and by B3-bases at the 6-311G(2d,p) level they have the same IR intensity, in agreement with the experimental data in gas phase.

The very strong IR band [15] at 1619 cm^{-1} was selected as representative of the β_s scissors deformation, although other bands with lower intensity as 1628 and 1611 cm^{-1} have also been assigned. This mode appears strongly coupled with the 8a mode. This fact leads, as discussed above, to a small difference in the displacement vector and in the wavenumber of both modes, which sometimes appear interchanged by the different methods and basis sets. Thus, by B3LYP/6-31G** the β_s mode is better identified in the computed wavenumber at 1658 cm^{-1}, with very weaker intensity than in the calculated wavenumber at 1677cm^{-1} with strong intensity. By contrast, with the 6-31G* and 6-311G(2d,p) basis set the β_s mode is better identified in the computed wavenumber with stronger intensity and higher wavenumber than the weaker and lower wavenumber that corresponds to mode 8a. These features can be observed with other methods.

The rocking mode, denoted as r or β_s, was computed very low intensity, in agreement with the very weak band reported in solution [15] at 1054cm^{-1}. The exception is AM1, calculated with strong intensity at 1166cm^{-1}. This mode appears in general strongly coupled with the 18b ring mode; thus, its characterization and detection by the theoretical methods is difficult.

Scaled frequencies using an overall scale factor											
AM1	PM3	HF/ 6-31G**	MP2/ 6-31G*	BP86/ 6-31G**	BLYP/ 6-31G**	B3P86/ 6-31G**	B3LYP/ 6-31G*	B3LYP/ 6-31G**	B3PW91/ 6-31G**	(a) 4-21G*	(b) B3LYP/ 6-31G*
−199	**−171**	17	−37	49	34	47	3	31	51	−6	−16
10	29	3	−59	24	14	23	−9	11	26	−10	−18
33	19	18	1	−26	−4	−32	11	−25	−30	34	8
57	6	−24	54	−21	−18	−27	−16	−22	−26	−2	−9
−18	**305**	−37	**124**	−45	−25	−78	−25	−54	−77	−91	−78
−24	−53	−40	−14	33	33	11	−16	15	18	−42	−16
87	**145**	25	62	35	24	42	15.0	29.8	43	43	34

The most obvious deviation between the calculated and the experimental spectrum is the position of the bands associated with the strongly anharmonic NH_2 wagging vibration. The $W(NH_2)$ mode is calculated (except by AM1 and SAM1) as the strongest IR intensity band. However, experimentally this mode appears as a very broad band with weak-medium intensity. This broad width, partially ascribed to the inversion transitions of the NH_2 group, makes it difficult to clearly identify the fundamental mode and leads to discrepancies in its value [3, 19]. The wavenumber at 658 cm^{-1} was selected as ν^{exp}, corresponding to the transition $3 \leftarrow 1$ ($\psi_1^{as} \leftarrow \psi_0^{s}$), in agreement with FT-IR results [17] at 658.5 ± 2 cm^{-1} and by resonance fluorescence [37] at 655 cm^{-1}. The other bands attributed to the wagging mode at 669 and 665 cm^{-1} have not been assigned to any transition [18] and thus were not considered. This election differs from the pseudo-experimental wavenumber estimated at 541 cm^{-1} (by average of the $3 \leftarrow 1$ and $2 \leftarrow 0$ transitions) by Rauhut and Pulay [19], 541.6 cm^{-1} by Niu et al. [3] and Castellá-Ventura and Kassab [6], and 670 cm^{-1} by Varsànyi [44]. The large differences observed in Table IX are a consequence of the badly calculated inversion ω angle. E.g., by PM3 and SAM1, the ω angle at 49.46 and 31.49°, respectively, differ from the 43.6° reported by ED [12], leading to the largest error. In contrast, by B3LYP/6-311G(2d,P) the value is the closest to the experimental and thus the lowest difference is found.

C_2 symmetry for the NH_2 group gives a $\tau(NH_2)$ torsional band not allowed by the IR selection rules. However, torsional bands were detected in the spectra of aniline [15, 17] and their derivatives [41, 54], because [17, 55] they are combinations of the torsion and inversion vibrations (transit $0 \rightarrow 1$), which are active in infrared. Thus, the value of 277.3 cm^{-1} deduced by Larsen et al. [17] was chosen instead of the 216 cm^{-1} by Evans [15] for the first overtone of this mode in vapor phase at 420 cm^{-1}. Our election has been followed by Rauhut and Pulay [19], while Castellá-Ventura and Kassab [6] considered 216 cm^{-1} and Niu et al. [3] 210 cm^{-1}. Song et al. [47] fail in the characterization of this mode, calculating at 411 cm^{-1}(instead of mode 16a), and thus related with the experimental band at 415 cm^{-1}.

Following the similar scheme of scaling described above with the ring modes, Table IX shows the absolute error in the calculated and in the scaled wavenumbers of Table VIII. Analogously, the BLYP method gives the best-calculated wavenumbers, while in the scaled wavenumbers with an overall factor it is B3LYP/6-31G*. The drastic reduction of the error with the scaling in HF, MP2, and B3-based methods is noted, although in some cases, especially in MP2, it remains large. Scale equations were determined to improve the accuracy (Table X). In general, a remarkable reduction of the error is obtained, ~40%, compared with the use of an overall scale factor. The reduction is noticeable with MP2, although it continues to be large. The best results are obtained with HF, using 6-31G* basis set or higher, as well as with B3LYP, using 6-31G* or 6-31G(2d,p). However, the rms errors are larger than those of Table VIII, mainly as a consequence of the relatively strong deviation for the wagging and

TABLE X

Scaling equations $\nu^{scaled} = a + b \cdot \omega^{calculated}$ for the NH_2 modes.

Methods	a	b	Methods	a	b
Semiempirical			Density functional		
MNDO	−122.16	0.9890	SVWN/6-31G**	98.49	0.9408
AM1	−46.03	1.0012	SLYP/6-31G**	97.42	0.9539
PM3	−100.90	1.0192	BP86/6-31G**	44.33	0.9699
SAM1	77.87	0.9583	BLYP/6-31G**	31.27	0.9791
			B3P86/6-31G*	33.03	0.9434
SCF and post-SCF			B3P86/6-31G**	57.39	0.9318
HF/6-31G*	22.72	0.8934	B3LYP/6-31G*	21.28	0.9555
HF/6-31G**	40.28	0.8846	B3LYP/6-31G**	44.52	0.9441
HF/6-31++G**	45.88	0.8833	B3LYP/6-311G(2d,p)	24.50	0.9572
MP2/6-31G*	−27.45	0.9614	B3PW91/6-31G**	56.81	0.9325

torsion modes. Our calculations, ab initio or semiempirical, are based on the harmonic model and thus are unable to take into account the anharmonicity of modes as $\omega(NH_2)$ and $\tau(NH_2)$, although the use of scaling equation partially reduces the error.

With remarkably large errors in the semiempirical methods, the best appears to be AM1 and the worst MNDO. Poor results are also obtained with SVWN and SLYP. In these methods, in MP2, and in the semiempiricals the error is largely inherent in the modes themselves and the wavenumbers need to be scaled using scale factors for each mode. For this purpose, Table XI lists these scale factors. They can also somewhat correct the underestimation predicted for the wagging mode with the other two scaling procedures, about 20 cm^{-1} with the best methods.

The results obtained at the B3LYP/6-31G** level in four aniline derivatives are shown in Table XII. For comparison purposes, the absolute error is shown for the three-scaled procedures. The rms error, MAD, and SD are shown in Table XIII.

It is noted that with the increment of the coupling with the ring modes, the transferability of the scale factors or the scale equations decrease and the errors increase. Thus, aniline, with only the NH_2 group substituted on the benzene, has the lowest error. *P*-fluroaniline, *P*-aminophenol, and *p*-toluidine with two substitutents groups have greater error. The experimental spectra of these compounds are in vapor phase and are comparable with our theoretical calculations; however, p-aminobenzoic acid is in solid or solution phase, and therefore has the largest error.

It was observed that the procedure with specific scale factors represents a remarkable improvement of the scaled wavenumbers over the scaling equation and these over the single overall factor procedure, at the B3LYP/6-31G** level being about 30% in the rms error. Thus, it should be the procedure recommended of scaling if a high degree of accuracy in the scaled wavenumbers is required.

Summary and Conclusion

With the goal of determining a quantum mechanical treatment that can be applied to large aromatic amines, the equilibrium geometries and the harmonic wavenumbers for aniline, obtained from various semiempirical and ab initio methods, have been compared with experimental data.

The stable structure of the two possible inversion conformers on the $-NH_2$ group has the N atom and two H atoms of the amino group on opposite sides of the ring plane. The special characteristic of the amino group is more accurately reproduced by AM1 and B3LYP/6-31G**, and much better than HF/6-31G* or the sophisticated MP2/6-31G*. In general, the values of the geometric parameters calculated were within the range of the mean absolute errors reported with these methods.

In the barrier height the C–N bond is slightly lengthened in the torsion and shortened in the inversion, while the C2–C–N is closer in the torsion and almost unchanged in the inversion. A remarkable increase of the inversion angle ω, a closing of the HNH angle and a decrease of the tilt ε characterize the torsion. The relation is almost linear with

TABLE XI

Specific scale factors ν^{exp}/ω^{cal} recommended to be used for the amino group vibrations.

Mode	AM1	PM3	SAM1	HF/6-31G**	MP2/6-31G*	SVWN 6-31G**	SLYP/6-31G**	BP86/6-31G**	BLYP/6-31G**	B3P86/6-31G**	B3LYP/6-31G*	B3LYP/6-31G**	B3LYP/6-311G (2d,p)	B3PW91/6-31G**
ν_{as}	1.0107	1.0261	0.9960	0.8949	0.9534	0.9626	0.9755	0.9777	0.9848	0.9431	0.9606	0.9529	0.9625	0.9436
ν_s	0.9791	0.9680	0.9644	0.8985	0.9598	0.9710	0.9847	0.9844	0.9904	0.9494	0.9640	0.9582	0.9644	0.9500
β_s	0.9342	0.9648	1.0144	0.8891	0.9429	1.0195	1.0332	1.0075	0.9969	0.9753	0.9549	0.9765	0.9730	0.9753
r	0.9039	0.9705	0.9934	0.9197	0.8978	1.0203	1.0323	1.0115	1.0115	0.9805	0.9761	0.9823	0.9847	0.9814
W	0.9806	0.6667	1.3623	0.9634	0.8820	1.4687	1.5023	1.1286	1.1040	1.1267	1.0405	1.0912	1.0341	1.1248
τ	1.0464	1.2109	0.9274	1.0625	1.1048	0.8253	0.8228	0.9400	0.9497	0.9337	0.9699	0.9497	0.9497	0.9337

TABLE XII

Vibrational wavenumbers of the -NH_2 group at B3LYP/6-31G level, experimental ones, and error obtained (in cm^{-1}) in the scaled values with the three procedures of scaling.**

	p-fluoroaniline					*p*-aminophenol					*p*-toluidine					*p*-aminobenzoic acid				
	Frequencies		Absolute error[a]			Frequencies		Absolute error[a]			Frequencies		Absolute error[a]			Frequencies		Absolute error[a]		
Mode	Cal.	Exp.	(1)	(2)	(3)	Cal.	Exp.	(1)	(2)	(3)	Cal.	Exp.	(1)	(2)	(3)	Cal.	Exp.	(1)	(2)	(3)
ν_{as}	3667.8	3498[b]	28	9	−3	3656.4	3481[b]	34	16	3	3667.6	3489[b]	37	18	6	3699.8	3500[f]	57	37	26
ν_s	3564.0	3415[b]	11	−6	0	3554.5	3402[b]	15	−2	4	3562.9	3405[b]	20	3	9	3587.8	3410[f]	39	22	28
β_s	1662.9	1630[c]	−31	−16	−6	1663.8					1661.9	1622[e]	−24	−9	1	1659.5	1622[g]	−27	−11	−1
r	1087.0	1078[c]	−33	−7	−10	1091.0	1095[e]	−46	−20	−23	1099.5					1077.5	1073[g]	−37	−11	−15
W	617.5	679.9[d]	−62	−53	−6	647.7	650?[e]				615.1	684.5[d]	−68	−59	−13	476.2	553[e]	−76	−59	−33
τ	262.0	245[d]	17	47	4	236.0					279.8					354.5	306?[g]			

[a] $\Delta(\nu^{scaled} - \nu^{exp})$, where ν^{scaled} is: (1) With an overall scale factor. (2) With a scaling equation. (3) With specific scale factors for each mode.
[b] In vapor phase, Ref. 58.
[c] Infrared, Ref. 56.
[d] In vapor phase, Ref. 59.
[e] Infrared, Ref. 44.
[f] In CCl_4, Ref. 60.
[g] Infrared, Ref. 57.

TABLE XIII

Errors obtained in the calculated and scaled wavenumbers of the amino group in several aniline derivatives at the B3LYP/6-31G level.**

	Calculated wavenumbers			Scaled wavenumbers with an overall factor			Scaled wavenumbers with the scaling equations			Scaled wavenumbers with specific scale factors		
Molecules	rms	MAD	SD	rms	MAD	SD	rms	MAD	SD	rms	MAD	SD
aniline	97.7	75.0	62.6	29.8	26.3	14.0	26.0	19.7	17.0	—	—	—
p-fluoroaniline	97.0	73.3	63.4	34.4	30.3	16.2	30.1	23.0	19.4	5.7	4.8	3.1
p-aminophenol	133.8	40.0	66.3	34.2	31.7	12.8	14.8	12.7	7.7	13.5	10.0	9.2
p-toluidine	125.9	111.5	58.4	41.7	37.2	18.8	31.2	22.2	21.9	8.5	7.2	4.4
p-aminobenzoic acid	125.7	99.2	77.2	50.3	47.2	17.3	33.4	28.0	18.2	23.6	20.6	11.4

ω. By the HF and MP2 methods, the inversion barrier of each is higher than by DFT methods, while the torsional barrier is remarkably lower. The maximum optimum *tilt* angle appears for torsional angles around 30–45°.

The ring modes were identified for the different methods by the value of the displacement vectors, in addition to their direction reported in the literature. The values differ drastically from those determined in the benzene molecule. The differences in the characterization by the various methods were analyzed. Depending on the method used, several modes drastically change their nature, e.g., modes 12 and 14.

The calculation and analysis of the IR spectrum leads to a reassignment of several fundamentals. The theoretical methods fail to predict the IR intensity, giving as the most intense that corresponding to the wagging ω (NH_2) mode, in contrast to its weak-medium intensity observed experimentally. However, in the other bands the relative intensities are comparable with our theoretical calculations.

The accuracy of the methods in calculating the wavenumber of the benzene ring modes was determined. For the C–H stretching region, the best calculated wavenumbers were those with PM3, while for the entire spectrum was the BLYP method and with the 6-31G* basis set or higher. No advantage was demonstrated with SAM1 over the other semiempirical methods, which fail in the predicted wavenumbers. The calculations at the HF level failed to give the observed experimental pattern, although the inclusion of electron correlation slightly improved the values. DFT methods have shown a more reliable prediction for the calculated wavenumbers than with the expensive HF and MP2 methods.

To improve the calculated wavenumbers, two new procedures for scaling the wavenumbers are proposed. The scaling equations procedure gives rise to a more noticeable improvement in the predicted wavenumbers than when a single overall scale factor is used. A new improvement is again obtained if different correction factors are used for different types of vibrations. The total mean deviation of the HF-, B-, and B3-based wavenumbers after scaling is only $\sim$10 cm^{-1}. In comparison with the scaling of the force constant, our procedures lead to easier and more precise prediction for specific characteristic wavenumbers of special interest.

The semiempirical methods fail dramatically for modes strongly coupled with the substituent, e.g., modes 8a, 8b, and 20a, and for modes badly characterized, e.g., mode 1. The use of scaling procedures partially corrects the failure.

For the computed wavenumbers of the semiempirical methods it is not recommended to use a single overall scale factor or a scaling equation; instead, specific scale factors for each mode should be used. The density functional wavenumber has more reliable predictions than the MP2 wavenumbers, and they are obtained at significantly less cost. If the wavenumbers are scaled with specific scale factors, the HF and B3-based methods lead to the best results.

References

1. Wolf, A.; Voets, U.; Scmidtke, H-H. Theoret Chim Acta 1980, 54, 229.

2. Niu, Z.; Bogges, J. E. J Mol Struct (Theochem) 1984, 109, 381.
3. Niu, Z.; Dunn, K. M.; Boogs, J. E. Mol Phys 1985, 55, 2, 421.
4. Wang, Y.; Saebø, S.; Pittman, C. U. J Mol Struct (Theochem) 1993, 281, 91.
5. Jiang, J. C.; Lin, C. E. J Mol Struct (Theochem) 1977, 392, 181.
6. Castellá-Ventura, M.; Kassab, E. Spectrochim Acta 1994, 50A, 1, 69.
7. Gorse, A-D.; Pesquer, M. J Mol Struct (Theochem) 1993, 281, 21.
8. Bock, C. W.; George, P.; Trachtman, M. Theor Chim Acta 1986, 69, 235.
9. Allinger, N. L.; Yan, L.; Chen, K. J Comput Chem 1994, 15, 12, 1321.
10. Roussy, G.; Nonal, A. J Mol Spectrosc 1986, 118, 180.
11. Lister, D. G.; Tyler, J. K.; Hog, J. H.; Larsen, N. W. J Mol Struct 1974, 23, 253.
12. Schultz, G.; Portalone, G.; Ramondo, F.; Domenicano, A.; Hargittai, I. Struct Chem 1996, 7, 1, 59.
13. Fukuyo, M.; Hirotsu, K.; Higuchi, T. Acta Crystallogr 1982, 38B, 2, 640.
14. Alcolea Palafox, M.; Melendez, F. J. J Mol Struct (Theochem) 1999, 493, 171.
15. Evans, J. C. Spectrochim Acta 1960, 16, 428.
16. Tripathi, G. N. R. J Chem Phys 1980, 73, 11, 5521.
17. Larsen, N. W.; Hansen, E. L.; Nicolaisen, F. M. Chem Phys Lett 1976, 43, 584.
18. Kydd, R. A.; Krueger, P. J. Chem Phys Lett 1977, 49, 3, 539.
19. Rauhut, G.; Pulay, P. J Phys Chem 1995, 99, 3093.
20. Meyer, W.; Pulay, P. Theor Chem Acta 1974, 32, 253.
21. (a) Hameka, H. F.; Famini, G. R.; Jensen, J. O.; Newhouse, E. I. Gov Rep Announce Index 1990, 90, 13; (b) Hameka, H. F.; Famini, G. R.; Jensen, J. O.; Jensen, J. L. Gov Rep Announce Index 1991, 91, 15.
22. Alcolea Palafox, M. Int J Quantum Chem 2000, 77, 661.
23. AMPAC 5.0, Semichem, Shawnee, Kansas.
24. Frisch, M. J.; Trucks, G. W.; Schlegel, H. B.; Scuseria, G. E.; Robb, M. A.; Cheeseman, J. R.; Zakrzewski, V. G.; Montgomery Jr, J. A.; Stratmann, R. E.; Burant, C.; Dapprich, S.; Millam, J. M.; Daniels, J. D.; Kudin, K. N.; Strain, M. C.; Farkas, O.; Tomasi, J.; Barone, V.; Cossi, M.; Cammi, R.; Mennucci, B.; Pomelli, C.; Adamo, C.; Clifford, S.; Ochterski, J.; Petersson, G. A.; Ayala, P. Y.; Cui, Q.; Morokuma, K.; Rega, N.; Salvador, P.; Dannenberg, J. J.; Malick, D. K.; Rabuck, A. D.; Raghavachari, K.; Foresman, J. B.; Cioslowski, J.; Ortiz, J. V.; Baboul, A. G.; Stefanov, B. B.; Liu, G.; Liashenko, A.; Piskorz, P.; Komaromi, I.; Gomperts, R.; Martin, R. L.; Fox, D. J.; Keith, T.; Al-Laham, M. A.; Peng, C. Y.; Nanayakkara, A.; Challacombe, M.; Gill,. P. M. W.; Johnson, B.; Chen, W.; Wong, M. W.; Andres, J. L.; Gonzalez, C.; Head-Gordon, M.; Replogle, E. S.; Pople, J. A. Gaussian 94, Gaussian Inc, Pittsburgh PA, 1995.
25. Dewar, M. J. S.; Zoebisch, E. G.; Healy, E. F.; Stewart, J. J. P. J Am Chem Soc 1985, 107, 3902.
26. Stewart, J. J. P. J Comp Chem 1989, 10, 2, 209, 221.
27. Dewar, M. J. S.; Jie, C.; Yu, J. Tetrahedron 1993, 49, 23, 5003.
28. Becke, A. D. Phys Rev 1988, A38, 3098.
29. Becke, A. D. J Chem Phys 1992, 97, 9173; 1993, 98, 5648.
30. Perdew, J. P. Phys Rev 1986, B33, 8822.
31. Lee, C.; Yang, W.; Parr, R. G. Phys Rev 1988, B37, 785.
32. Perdew, J. P.; Wang, Y. Phys Rev 1992, B45, 13244.
33. Johnson, B. G.; Gill, P. M. W.; Pople, J. A.; J Chem Phys 1993, 98(7), 5612.
34. Smith, D. A.; Ulmer C. W. II; Gilbert, M J. J Comput Chem 1992, 13, 5, 640.
35. Radhakrishnan, T. P.; Agranat, I. Struct Chem 1991, 2, 107.
36. Pyka, J.; Kreglewski, M. J Mol Spectrosc 1985, 109, 207.
37. Quack, M.; Stocburger, M. J Mol Spectrosc 1972, 43, 87.
38. Chernoff, D. A.; Rice, S. A. J Chem Phys 1979, 70, 2511.
39. Brand, J. C. D.; Willians, D. R.; Cook, T. J. J Mol Spectrosc 1966, 20, 359.
40. Bludskỳ, O.; Šponer, J.; Leszczynski, J.; Špirko, V.; Hobza, P. Chem Phys 1996, 105, 24, 11042.
41. (a) Alcolea Palafox, M. Spectrochim Acta 1988, 44A, 12, 1465; (b) Alcolea Palafox, M. Rev Roum Chim 1989, 34, 8, 1667.
42. Hamilton, J. A.; Sabesan, M. N. Carbohydr Res 1982, 102, 31.
43. Alcolea Palafox, M. Asian J Phys 1997, 6, 4, 477.
44. Varsànyi, G. In Assignment for Vibrational Spectra of Seven Hundred Benzene Derivatives; Adam Hilger: London, 1974, p 81.
45. Wilson, E. B. Phys Rev 1934, 45, 706.
46. Scherer, J. R. Spectrochim Acta 1963, 19, 601.
47. Song, X.; Yang, M.; Davidson, E. R.; Reilly, J. P. J Chem Phys 1993, 99, 5.
48. Seeger, D. M.; Korzeniewski, C.; Kowalchyk, W. J Chem Phys 1991, 95, 6871.
49. Alcolea Palafox, M. Recent Res Dev Phys Chem 1998, 2, 213.
50. Scott, A. P.; Radom, L. J Phys Chem 1996, 100, 16502.
51. Miller, M. D.; Jensen, F.; Champman, O. L.; Houk, K. N. J Phys Chem 1989, 93, 4495.
52. Raghavachari, K.; Trucks, G. W.; Pople, J. A.; Replogle, E. Chem Phys Lett 1989, 158, 207.
53. (a) Alcolea Palafox, M. J Mol Struct (Theochem) 1991, 236, 161; (b) Alcolea Palafox, M.; Melendez, F. J. J Mol Struct (Theochem) 1999, 459, 239.
54. (a) Alcolea Palafox, M. Rev Roum Chim 1996, 41, 3-4, 223; (b) Alcolea Palafox M. Indian J Pure Appl Phys 1991, 3-4, 5842; (c) Alcolea Palafox, M. Spectrosc Lett 1997, 30, 8, 1495.
55. Alcolea Palafox, M. J Mol Struct 1988, 175, 81.
56. (a) Borisenko, V. E.; Tuchkova, E. I. Spectrosc Lett 1994, 27, 6, 741; (b) Borisenko, V. E.; Greseva, E. I.; Dukhnova, E. V.; Nachena, I. V. Mol Struct 1994, 324, 199.
57. (a) Sanchez de la Blanca, E.; Núñez, J. L.; Martínez, P. An Quim Ser A 1986, 82, 3, 480; (b) Sanchez de la Blanca, E. PhD Thesis, Madrid, 1986.
58. Nyquist, R. A. Appl Spectrosc 1993, 47, 4.
59. Kydd, R. A.; Krueger, P. J. J Chem Phys 1978, 69 (2), 827; 1980, 72 (1), 280.
60. Théorêt, A. Spectroschim Acta 1971, 27A, 11.